

ARDHI UNIVERSITY



**COMPUTATION OF DYNAMIC AND ORTHOMETRIC HEIGHTS AND
ANALYSIS OF NORMAL HEIGHTS FOR TAREF11 CONTROLS USING
TZQ17 AND XGM2019e_5540 GEOPOTENTIAL MODEL**

A Case Study of TAREF11 control points

MAPUNDA, VICTOR P

BSc Geomatics

Dissertation

Ardhi University, Dar es Salaam

July, 2023

COMPUTATION OF DYNAMIC AND ORTHOMETRIC HEIGHTS AND ANALYSIS OF
NORMAL HEIGHTS FOR TAREF11 CONTROLS USING TZQ17 AND XGM2019e_5540
GEOPOTENTIAL MODEL

A Case Study of TAREF11 control points

MAPUNDA, VICTOR PAUL

A Dissertation Submitted to the Department of Geospatial Sciences and Technology in Partially
Fulfilment of the Requirements for the Award of Bachelor of Science in Geomatics (BSc. GM)
of Ardhi University

CERTIFICATION

The undersigned certify that they have read and hereby recommend for acceptance by the Ardhi University dissertation titled **“Computation of Dynamic and Orthometric Heights and Analysis of Normal Heights for TAREF11 Controls Using TZQ17 and XGM2019e_5540 Geopotential Model”** in partial fulfillment of the requirements for the award of degree of Bachelor of Science in Geomatics at Ardhi University.

.....

Ms. REGINA V. PETER

Supervisor

Date.....

DECLARATION AND COPYRIGHT

I, **MAPUNDA, VICTOR PAUL** hereby declare that, the contents of this dissertation are the results of my own findings through my study and investigation, and to the best of my knowledge they have not been presented anywhere else as a dissertation for diploma, degree or any similar academic award in any institution of higher learning.

.....

MAPUNDA, VICTOR PAUL

22828/T.2019

(Candidate)

Copyright ©1999 This dissertation is the copyright material presented under Berne convention, the copyright act of 1999 and other international and national enactments, in that belief, on intellectual property. It may not be reproduced by any means, in full or in part, except for short extracts in fair dealing; for research or private study, critical scholarly review or discourse with an acknowledgement, without the written permission of the directorate of undergraduate studies, on behalf of both the author and Ardhi University.

ACKNOWLEDGEMENT

I wish to register my profound gratitude to The Almighty Allah for the guidance, protection and grace throughout my study.

Furthermore, I extend my special regards and appreciations to my supervisor, Ms. Regina V. Peter for the continuous support, patience, motivation and immense knowledge. Her guidance helped me in all time of research and writing of this dissertation. May God bless her work and contribution abundantly.

I would also like to express my deepest gratitude to my family, friends and to all those who have directly and indirectly guided me in writing this dissertation, your valuable comments and suggestions are highly appreciated. I am forever thankful for the unconditional love and support throughout the entire dissertation process and every day.

DEDICATION

To the experience we never expected,

and the path that were redirected,

To the friends and family, we found along the way,

*To my mother Dorothy Alphonso and my late father Paul E. Mapunda for their endless love,
support and encouragement.*

ABSTRACT

Height system is a one-dimensional coordinate system used to express the metric distance (height) of a point above a reference surface along a well-defined path. There are two types of height systems, these are Geometrical and physical height system such as orthometric, normal and dynamic heights. Physical height systems based on orthometric heights use the geoid as reference surface while normal height use quasigeoid. Dynamic heights on the other hand are just geopotential number scaled into metric unit.

This dissertation aims at computation of dynamic and orthometric heights and analysis of normal heights for TAREF11 controls using TZQ17 and XGM2019e_5540 geopotential model along with validation of orthometric and normal heights using TZG17 and a strict formula for geoid to quasi-geoid separation (GQS) respectively. The evaluation and analysis was done by comparing the difference of orthometric heights computed by XGM2019e_5540 and TZG17 as well as normal heights of TZQ17 and XGM2019e_5540 with those of a strict formula for geoid-quasi geoid separation. Data used for determination, evaluation and analysis of dynamic, orthometric and normal heights are geopotential numbers, mean normal gravity, mean gravity, ellipsoidal heights, height anomalies, Bouguer gravity anomalies, geoid undulation and GPS orthometric height.

Comparison was done by statistical analysis of the difference between the two height approaches i.e. normal height computed using XGM2019e_5540 and TZQ17 or orthometric height computed by XGM2019e_5540 and TZG17. Assessment of the orthometric and normal height was done based on statistical analyses in which a test was conducted at 95% and the results showed that the residual between normal height computed using geopotential number and a strict formula have a SD of 9mm and those computed by TZQ17 and a strict formula have a SD of 1.2cm. Also, the residual between the orthometric height computed by using XGM2019e_5540 and TZG17 have a SD of 6mm and those computed by GPS levelling and XGM2019e_5540 have a SD of 1.2cm.

KEYWORDS: TZQ17 quasi-geoid model, TZG17 geoid model, Geopotential number, TAREF11, Dynamic height, Orthometric height, Normal height, a strict formula and Geoid to quasigeoid separation.

TABLE OF CONTENTS

CERTIFICATION	ii
DECLARATION AND COPYRIGHT	iii
ACKNOWLEDGEMENT	iv
DEDICATION.....	v
ABSTRACT	vi
LIST OF FIGURES	xi
LIST OF TABLES	xii
LIST OF ABBREVIATIONS	xiii
CHAPTER ONE	1
INTRODUCTION.....	1
1.1 Height System	1
1.2 Statement of the problem	4
1.3 Main objective.....	5
1.3.1 Specific objectives	5
1.4 Research questions	5
1.5 Significance of the research	6
1.6 Beneficiaries of the research	6
1.7 Scope/limitations of the research	6
1.8 Study Area.....	6
1.9 Research Outline	7
CHAPTER TWO	9
LITERATURE REVIEW	9
2.1 Overview of Tanzania spatial reference system.....	9
2.2 Physical Height System.....	11

2.2.1 Geopotential number (c).....	11
2.2.2 Orthometric height.....	13
2.2.3 Normal height.....	15
2.2.4 Dynamic height.....	16
2.3 Overview of Global Geopotential Models (GGMs).....	17
2.4 XGM2019e.....	18
2.5 WGM12.....	18
2.6 Overview of Geoid and Quasi-geoid.....	19
2.6.1 A strict formula for Quasigeoid-Geoid separation ($N - \zeta$).....	20
CHAPTER THREE	23
METHODOLOGY	23
3.1 Determination of the Actual Gravity Potential of TAREF11 controls.....	23
3.2 Determination of the Geopotential Number.....	25
3.3 Extraction of height anomaly (ζ_p) from TZQ17 quasi-geoid.....	26
3.4 Extraction of geoid undulation(N) from TZG17 geoid model	27
3.5 Computation of Normal Gravity	27
3.6 Computation of mean normal gravity	28
3.7 Computation of mean gravity.....	28
3.8 Computation of Normal Heights Using Geopotential Numbers	28
3.9 Computation of Normal Heights Using TZQ 17 quasi-geoid	28
3.10 Computation of Normal height by a strict formula	29
3.11 Computation of Orthometric height from geopotential number	30
3.12 Computation of Orthometric height from TZG17.....	30
3.13 Computation of Dynamic height from geopotential number	30
3.14 Data used and its sources	30

3.14.1 Software.....	31
CHAPTER FOUR.....	33
RESULTS AND ANALYSIS	33
4.1 Results	33
4.1.1 Extracted surface gravity and actual gravity potential of TAREF11 control points	33
4.1.2 Computed Geopotential numbers of TAREF11 Control points	34
4.1.3 Extracted height anomaly (ζ_p) of TAREF11 controls from TZQ17 quasi-geoid model	35
4.1.4 Extracted geoid undulation (N) of TAREF11 control points from TZG17 geoid model	36
4.1.5 Computed normal gravity of TAREF11 control points.....	37
4.1.6 Computed mean normal gravity and mean gravity of TAREF11 control points	38
4.1.7 Computed normal heights of TAREF11 control points Using Geopotential numbers.	39
4.1.8 Computed normal heights of TAREF11 control points using TZQ17 quasi-geoid model	40
4.1.9 Computed normal heights of TAREF11 control points using a strict formula	41
4.1.10 Computed orthometric height of TAREF11 control points using geopotential number	42
4.1.11 Computed orthometric height of TAREF11 control points using TZG17 geoid model	43
4.1.12 Computed dynamic height of TAREF11 control points using geopotential number .	44
4.2 Statistical analysis of Normal heights differences of TAREF11 controls	45
4.3 Statistical analysis of Orthometric heights differences of TAREF11 controls	46
4.4 Discussion of the results.....	47
CHAPTER FIVE	49
CONCLUSION AND RECOMMENDATION	49

5.1 Conclusion.....	49
5.2 Recommendations	49
REFERENCES	50
APPENDICES	54
APPENDIX 1: CORS and Zero order data extracted from XGMe2019 model.....	54
APPENDIX 2: FIRST order data extracted from XGMe2019 model	56
APPENDIX 3: SECOND order data extracted from XGMe2019 model	58
APPENDIX 4: Bouguer gravity anomalies extracted from WGM12 model	60
APPENDIX 5: Computed Geopotential numbers of TAREF11 control points.....	62
APPENDIX 6: Extracted height anomaly (ζ_p) and Geoid undulations (N) of TAREF11 control points from TZQ17 quasi-geoid model and TZG17 geoid model	64
APPENDIX 7: Computed normal gravity of TAREF11 control points.....	66
APPENDIX 8: Computed mean normal gravity and mean gravity of TAREF11 control points	68
APPENDIX 9: Computed normal heights of TAREF11 control points using Geopotential numbers	70
APPENDIX 10: Computed Normal Heights of TAREF11 control points using TZQ 17 quasi-geoid model	72
APPENDIX 11: Computed Normal Heights of TAREF11 control points using a strict formula for geoid to quasi-geoid separation	74
APPENDIX 12: Computed orthometric height of TAREF11 control points using Geopotential number.....	76
APPENDIX 13: Computed orthometric height of TAREF11 control points using TZG17 geoid model.....	78
APPENDIX 14: Computed dynamic height of TAREF11 control points using Geopotential number.....	80

LIST OF FIGURES

Figure 1.1: Physical and geometric heights with their respective reference surfaces.	1
Figure 1.2: Distribution of TAREF11 control points used in this research study.	7
Figure 2.1: levelling and orthometric height (Hofmann-Wellenhof & Helmut, 2005)	12
Figure 2.2: Definition of Orthometric height (Featherstone & Kuhn, 2006).....	13
Figure 2.3: Normal orthometric height and normal height (Featherstone & Kuhn, 2006).....	16
Figure 2.4: Complete Bouguer gravity anomaly over Tanzania mainland surface	19
Figure 2.5: Relationship of the Quasi-geoid, geoid and the reference ellipsoid (Peter, 2018).	20
Figure 3.1: A GUI of Graf lab software that was used in computations of actual gravity potential on the surface of the earth.	24
Figure 3.2: Sample of extracted Gravity and Gravity potential from XGM2019e_5540 GGM... ..	25
Figure 3.3: Inputs and output section for extraction of height anomalies	26
Figure 3.4: Inputs and output section for extraction of geoid undulation.....	27
Figure 3.5: Inputs and output section for extraction of Bouguer gravity anomalies	29

LIST OF TABLES

Table 3.1: Data used in this research	31
Table 3.2: Software that was installed and its uses in this research.	32
Table 4.1: Computed actual gravity potentials of TAREF11 Control points	33
Table 4.2: Computed geopotential number values of TAREF11 Control points	34
Table 4.3: Extracted height anomaly (ζ_p) values of TAREF11 control points.....	35
Table 4.4: Extracted geoid undulation (N) values of TAREF11 controls from TZG17	36
Table 4.5: Computed normal gravity values of TAREF11 control points.....	37
Table 4.6: Computed mean normal gravity and mean gravity values of TAREF11 controls	38
Table 4.7: Computed Normal height of TAREF11 controls using Geopotential number	39
Table 4.8: Computed Normal heights of TAREF11 controls Using TZQ17	40
Table 4.9: Computed Normal height of TAREF11 control using strict formula.....	41
Table 4.10: Computed Orthometric height using geopotential number	42
Table 4.11: Computed Orthometric heights of TAREF11 controls from TZG17 geoid model ...	43
Table 4.12: Computed Dynamic heights of TAREF11 controls using geopotential number	44
Table 4.13: Statistic of computed normal heights of TAREF11 controls.....	45
Table 4.14: Statistical analysis of TAREF11 controls normal heights differences	45
Table 4.15: Statistic analysis of normal heights differences at 95% confidence interval.....	46
Table 4.16: Statistic of computed Orthometric heights of TAREF11 controls	46
Table 4.17: Statistical analysis of TAREF11 controls Orthometric heights differences	47
Table 4.18: Statistic analysis of orthometric heights differences at 95% confidence interval	47

LIST OF ABBREVIATIONS

ARC1960	Arc Datum Geodetic Network of 1960
BGI	Bureau Gravimetrique International
BM _s	Benchmark(s)
CGMW	Commission for the Geological Map of the World
CORS	Continuous Observation Reference Stations
d/o	Degree and Order
DORIS	Doppler Orbitography and Radio Positioning Integrated by Satellite
DoS	Directorate of Overseas Surveys
DTU	Technical university of Denmark
EGM08	Earth Gravity Model 2008
GEM	Goddard Earth Models
GGM _s	Global Gravitational Models
GNSS	Global Navigation Satellite System
GOS	Global Geodetic Observing System
GQS	Geoid to quasi-geoid separation
GPS	Global Positioning System
IAG	International Association of Geodesy
ICGEM	International Center of Global Earth Models
IGF	International Gravity Formula
ITRF	International Terrestrial Reference Frame
ITRS	International Terrestrial Reference Systems
IUGG	International Union of Geodesy and Geophysics

IUGS	International Union of Geological Sciences
JGM	Joint Gravity Models
LVD	Local Geopotential Vertical Datum
MATLAB	Matrix Laboratory
MSL	Mean Sea Level
NSRS	National Spatial Reference System
TAREF11	Tanzania Reference Frame 2011
TPLN	Tanzania Primary Levelling Network
TZG17	Tanzania Gravimetric Model of 2017
TZQ17	Tanzania Quasi-Geoid Model of 2017
VD	Vertical Datum
VLBI	Very Long Baseline Interferometry
WGM12	World Gravity Map 2012
XGM2019e	Experimental Gravity Model of 2019

CHAPTER ONE

INTRODUCTION

1.1 Height System

A height system is a one-dimensional coordinate system used to express the metric distance (height) of a point above a reference surface (i.e., the zero-height level) along a well-defined path. If the reference surface and the height are linked to equipotential surfaces and the plumb line of the Earth's gravity field, the height system is called physical height system. If the reference surface and the height do not depend on the Earth's gravity field, the height system is called geometric height system (Melitha, 2020). Figure 1.1 below shows the physical and geometric heights with their reference surface.

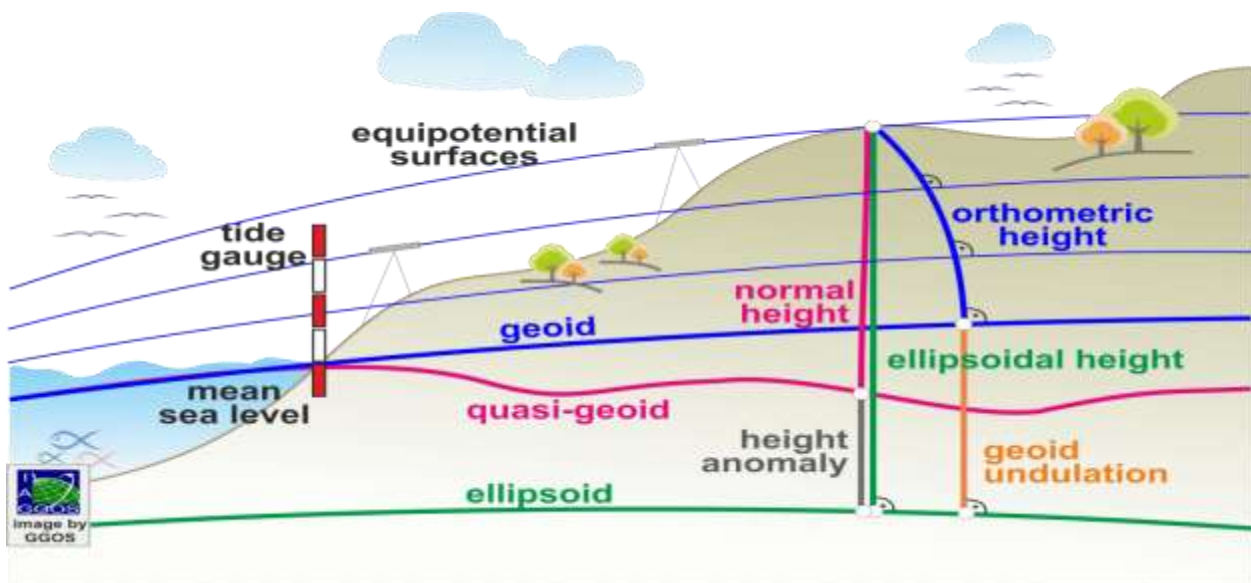


Figure 1.1: Physical and geometric heights with their respective reference surfaces.

For height to be considered as true height it should satisfy fundamental properties of a true measure of height system which are;

- i. Height must be unique
- ii. They must be sensitive to the flow of fluid I.e., fluid flow from region of higher potential to the one with lower potential.
- iii. Height should be a geometrical distance and therefore measured in meters i.e., they should have unit of length.

iv. Easy to compute

Depending on the gravity correction applied to levelling, different types of physical heights are distinguished: orthometric heights, normal heights, or dynamic heights. Physical height systems based on orthometric heights use the geoid as reference surface. The geoid is the equipotential surface that best fits the mean sea level while physical height systems based on normal heights use the quasi-geoid as reference surface. Orthometric and normal heights are widely used in the definition and realization of physical height systems, while dynamic heights are mainly employed to define the height coordinate in water bodies (e.g., large lakes) and some residual sets of tasks, mostly related to hydrodynamics and energetics of transporting mass such as construction of canals, dams and pipeline (Bedada, 2010).

Dynamic heights are just geopotential numbers, scaled into a metric unit. This system is most closely related to the system of geopotential numbers. Since the geopotential number is divided by a constant value, dynamic heights retain the same characteristics except that they have the dimension of length. Physical height systems based on orthometric heights use the geoid as reference surface. The geoid is the equipotential surface that best fits the mean sea level. Physical height systems based on normal heights use the quasi-geoid as reference surface. The quasi-geoid is close to the geoid but not an equipotential surface as the geoid is. The quasi-geoid deviates from the geoid in the same way as the normal heights deviate from the orthometric heights. They present differences on the millimeter to centimeter order at low elevations and may reach 1 m deviation in high mountains (Sadiq, Ahmad & Akhter, 2009). On the oceans, geoid and quasi-geoid as well as orthometric and normal heights practically coincide. The transformation between geometric and physical height systems is given by;

$$h = H + N \approx H^N + \zeta \dots\dots\dots (1.1)$$

where h is the ellipsoidal height, H and H^N are the orthometric and normal heights, respectively, N is the geoid undulation, and ζ is the height anomaly.

The realization of physical heights system is very difficult due to the facts that it requires enough knowledge about the gravity inside the earth's surface a good example is the orthometric height system. Thus, due to this problem a normal height system was developed by Molodensky (1945, 1948). This height system use quasigeoid as its vertical datum and it have a great advantage of being determined without knowledge of topographic density distribution (Foroughi et al., 2017).

Modernization of height systems and height reference networks is currently on going in many countries. This is among other reasons, driven by the increasing need to provide precise and well-defined height reference surfaces for GNSS leveling (Sjöberg, 2013). To obtain orthometric and normal heights values referred to any of vertical datum at a given point in Tanzania, it is possible to carry out spirit levelling from a benchmark and interpolate the real gravity value from Tanzania gravimetric network data. However, with the expressive technological development experienced in recent decades, new methods for obtaining altimetric data have gained projection supported by improvement of related observations and techniques (Delgado & Rodrigues, 2022).

In this context innumerable researchers have proposed the use of GNSS ellipsoidal heights in conjunction with data provided with Global Geopotential Models (GGMs) to obtain physical heights. In the context of physical heights obtained from GNSS/GGM integration there is the advantage of avoiding the costly and time-consuming spirit levelling procedure from some benchmark, especially in regions with lower and sparse station density. Global geopotential model (GGM) is set of spherical harmonic coefficients of the earth gravity potential of external type i.e., external to the MES as the bounding surface (Ulotu, 2009) , based on this research the GGM that will be used is XGM2019e which is a combined global gravity field model represented by spheroidal harmonics up to degree and order (d/o) 5540 (Zingerle et al., 2020).

Different researches have been conducted on the determination of different heights using global Geopotential models global and in Tanzania such as (Delgado & Rodrigues, 2022) used GNSS and a refined GGM (XGM2019e) to determine normal heights in the Imbituba Brazilian Vertical Datum and in the International Height Reference System. The research results showed that normal heights computed had an increased accuracy of 0.97m to 0.10m and 0.39 to 0.17 in both sub regions (SP1&SP2) respectively compared to that of Brazilian official normal heights. Although the calculated accuracies were below those desired by the IAG/ GGOS, the local modeling approach was more accurate than a national modeling approach.

Also, (Idrissa, 2022) computed, evaluated and analyzed normal heights of TPLN benchmarks using TZQ17 and geopotential number. Results showed that at 95% confidence interval there is significance difference of 5.4cm between the normal heights computed by geopotential number and that from TZQ17 quasi-geoid. Also, (Mushi, 2022) computed helmert orthometric height using XGM2019e_5540 GGM and assessment using normal orthometric height of TPLN benchmarks

with GPS/levelling in Tanzania. Results showed that normal orthometric height of TPLN deviates to large extent comparing to those of helmert's orthometric height.

Tanzania Primary Levelling Network (TPLN) is the Tanzania network for realization of orthometric height which was designed in the 1960's and implemented between 1961 and 1964 (Mayunga, 2016) and its establishment was based on the Tanga Tide Gauge (TG) station. Tanzania primary levelling network consist of fifty-three (53) Fundamental benchmarks made up on loops based on local mean sea level (Idrissa, 2022). The levelled orthometric heights in the TPLN were corrected for gravity effects on the basis of the normal gravity and for that reason Tanzania height system is a normal orthometric height in practice (Deus, 2007).

In Tanzania, all of previous researches worked only on orthometric and normal heights of TPLN benchmarks which have sparse network stations and several limitations such as not being compatible with the current space geodetic techniques such as GNSS, VLBI, and DORIS. However, Tanzania is into developing National Spatial Reference System (NSRS) and with development of TAREF11 reference frame and considering the advances in data caption and theory for geoid and quasigeoid determination as well as the available Global Geopotential Model there's a need for assessing the available TAREF11 orthometric heights using geopotential number. Also, computation of normal heights is inevitable as unlike orthometric heights does not require knowledge of internal topographic mass density distributions. Dynamic heights computation is also required since its mostly needed in some residual sets of tasks, mostly related to hydrodynamics and energetics of transporting mass such as construction of canals, dams and pipeline.

Therefore, this study will compute dynamic, orthometric and normal heights of TAREF11 control points using geopotential number along with its analysis and validation using TZG17 geoid model and a strict formula for geoid to quasigeoid separation respectively.

1.2 Statement of the problem

Most European states use M.S. Molodensky's concept of normal heights for their height systems with a quasigeoid model as the reference surface, while the rest of the world rely on orthometric heights with the geoid as the zero-level, Tanzania height system is orthometric height and normal orthometric height is the one in practice. In fact, both Tanzania geodetic and primary leveling network have several limitations which led to the development of the TAREF11 frame in 2010

observed through GNSS levelling. Since gravity corrections was not accounted in TAREF11 observations hence assessment of its orthometric heights accuracies using GGMs is necessary. Also, as step towards the realization of a unified global vertical frame, computation of normal height is also needed as both orthometric and normal height are needed for realization of physical height system. However, some residual sets of tasks, mostly related to hydrodynamics and energetics of transporting mass such as construction of canals, dams and pipeline still requires geopotential height to map level surfaces on or above the Earth's surface. Thus, dynamic height is also still needed since it's the only height sensitive to the flow of fluid.

1.3 Main objective

The main objective is to compute dynamic, orthometric and normal height of TAREF11 controls using Geopotential number from XGM2019e_5540 d/o and analysis of the normal heights computed by TZQ17 and those by XGM2019e_5540 geopotential model.

1.3.1 Specific objectives

The research will be conducted under the following specific activities that will yield to project main objective.

- i. To compute actual gravity potential of all TAREF11 control points from combined global gravity field model XGM2019_5540 and later computing component of geopotential number.
- ii. To compute mean gravity, normal gravity and mean normal gravity of TAREF11 points.
- iii. To compute the orthometric, dynamic and normal height from computed component of geopotential number and validation of orthometric heights by TZG17 geoid model.
- iv. Analysis of normal height from XGM2019e_5540 Geopotential model and TZQ17 with its validations using a strict formula for geoid to quasigeoid separation by statistical comparison of its results to check if they are significantly consistent.

1.4 Research questions

A few questions are posed prior to the research which include;

- i. What will be the significant consistent of orthometric height computed by geopotential number with those from GNSS levelling?

- ii. What will be the significant consistent of normal heights computed by XGM2019e_5540, a strict formula and those from TZQ17?
- iii. What will be the significant consistent of orthometric heights computed by XGM2019e_5540, GPS levelling and those from TZG17?

1.5 Significance of the research

- i. Determination of geopotential height system will help field surveyors and engineers in construction of structures which requires the potential to be evaluated on or above the Earth's surface.
- ii. The demand of height information from satellite user based on global position system (GPS) has increased, on determination of normal, orthometric and dynamic height by using geopotential number will reach their demand.
- iii. Tanzania is into developing National Spatial Reference System (NSRS) so the resolution of the height component could make TAREF11 essential in the Vertical Spatial Reference System

1.6 Beneficiaries of the research

The beneficiaries of this research are tending to be:

- Engineering construction industry.
- Surveying and mapping institutions.
- Researchers

1.7 Scope/limitations of the research

This study will focus on Computation of dynamic and orthometric heights and analysis of normal heights of TAREF11 controls using TZQ17 and XGM2019e_5540 Geopotential model as well validation of orthometric and normal heights by TZG17 and a strict formula respectively. The study will cover all TAREF11 control points.

1.8 Study Area

The research study area is Tanzania mainland across all TAREF11 control points. Its extent is 28° E to 42° E from the prime meridian and 1° to 12° south of the equator. There are over 600 TAREF11 control points including those of CORS, zero order, first order and second order. Figure 1.2 shows the distribution of TAREF11 controls used in this research

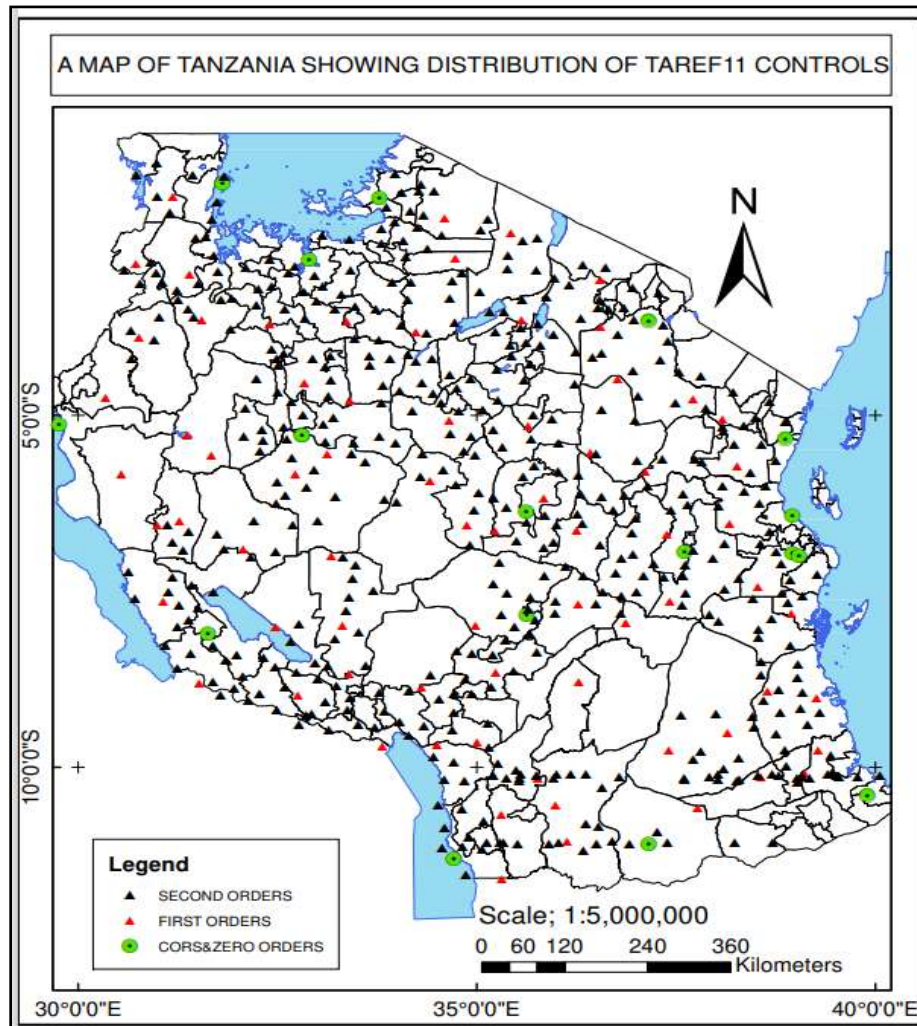


Figure 1.2: Distribution of TAREF11 control points used in this research.

1.9 Research Outline

This study is dedicated in computation of dynamic and orthometric heights and analysis of normal heights of TAREF11 controls using TZQ17 and XGM2019e_5540 Geopotential Model. Orthometric heights are computed from geopotential model and its validation by TZG17 geoid model. Also, the analysis and validation of normal heights from geopotential model and TZQ17 quasi-geoid model is done by a strict formula for geoid to quasigeoid separation through statistical comparison to see how significance are they. This study consists of five chapters as listed below;

Chapter one

This chapter gives the background overview of this research, Problem Statement, objectives of the research, significance of the research, beneficiary, study area, scope and Limitation of the research.

Chapter two

This chapter provides an overview of the TAREF11, Physical height system which consist of (normal heights, geopotential numbers orthometric heights and dynamic height), overview of the global geopotential models (GGMs) as well as Overview of Geoid and quasi-geoid.

Chapter three

This chapter describes the methodologies used to achieve the objectives, mathematical models and detailed description of all datasets required to achieve the objectives of the study.

Chapter four

This chapter present the results and discussion of the results.

Chapter five

This chapter present conclusion and recommendations from the conducted research. conclusion gives the summary of the research findings in view of the solution to research problem and attaining the main objectives while recommendation explain follow up after the research findings.

CHAPTER TWO

LITERATURE REVIEW

2.1 Overview of Tanzania spatial reference system

Spatial reference system provides a framework for defining locations on the surface of the Earth. There are two types of spatial reference systems, referred to as geographic coordinate systems and projected coordinate systems. Projected coordinate systems provide various mechanisms to project the Earth's spherical surface onto a two-dimensional planar surface for creating maps while a geographic coordinate system defines locations on the earth using a three-dimensional spherical surface that approximates the shape of the Earth. (Snyder, 1987). A geodetic datum is a reference point on the earth's surface from which spatial measurements are made. Geodetic datum constitutes of horizontal and vertical datum. Horizontal datum is used for describing a point on the earth's surface in latitude and longitude whereas vertical datum is used to specify vertical heights from a base of surface approximated using calculations of mean sea level.

Vertical Datum (VD) is a reference surface of zero elevation relative to which heights or depths are referred to. The Mean Sea Level (MSL) has been used extensively for a long time as VD all over the World. It is realized by averaging sea water levels over a minimum period of 18.6 years at a Tide Gauge (TG) station in a coastal area. By averaging the sea water levels over a long period, seasonal and periodical sea level fluctuations can be reduced to the minimum (Ulotu, 2015).

Tanzania, like most African countries, has an old and conventional geodetic network based on the 1880 Clarke modified ellipsoid, with its datum at Buffelsfontein, near Port Elizabeth-Cape Town, in the Republic of South Africa. The established reference ellipsoid initial geodetic objectives were to verify the size and shape of the Earth in the Southern Hemisphere and provide geodetic control for topographic maps and navigation charts. The network was then extended to other countries in central Africa of Zimbabwe and Democratic Republic of Congo. The Tanzanian 1950 arc datum control network was derived from the Republic of South Africa geodetic datum via Zimbabwe and since its establishment has never been validated to ascertain the extent of distortions. Like most of the conventional geodetic networks in other countries, the establishment and the densification methodology were done using traditional methods such as classical triangulation, trilateration and standard traversing (Mtakamaya, 2009). The network was proven to have several limitations which includes;

- i. It is not compatible with the current space geodetic techniques such as GNSS, VLBI, and DORIS.
- ii. The frame provides horizontal solutions only contrary to most positioning applications that require a 3D mapping reference frame.
- iii. The mapping frame was not homogenous within itself and neighboring countries mapping frames.

On the other hand, For the case of heights system, TPLN is the network for realization of orthometric heights in Tanzania. Tanzania Primary Levelling Network (TPLN) was designed in the 1960's and implemented between 1961 to 1964 and its establishment was based on the Tanga Tide Gauge (TG) station (Mayunga, 2016). Tanzania primary levelling network consist of fifty-three (53) Fundamental benchmarks made up on loops based on local mean sea level. The leveled height (orthometric height) is corrected for gravity effects on the basis of the normal gravity computed by means of international Gravity Formula ,1930 (Deus, 2007). The establishment of TPLN referred on the Tanga tide gauge benchmark at Tanga harbor whose Mean Sea level was used as reference. The value for the mean sea level (MSL) at Tanga harbor was deduced from tide gauge readings taken during a 28 months' period from August 1962 to November 1964, both months inclusive. The MSL was used to determine the elevation of the Reference Fundamental Benchmark then other land benchmarks were connected to the FBM through the observations of loops (Ulotu, 2015).

Tanzania TG based VD has a lot of limitations or deficiencies to qualify for the National VD. Some of the problems include the Mean Sea Level (MSL) establishment was based on the data which were observed for 2.3 years only instead of being observed for at least 18.6 years, MDT was not accounted for at Tanga TG station, effects of salinities, sea temperature, ocean currents and coast line configuration were not modelled and therefore the effects were not removed and hence displace tidal VD from geoid (Ulotu, 2009).

Also, during 1960's a model for geoid of Tanzania did not exist then a local MSL was used in place of the geoid surface. Thus, the existing TPLN based on Tanga tide gauge MSL as approximation to the correct vertical datum (geoid). Generally, the existing vertical datum of TPLN does not coincide with the geoid in Tanzania (Idrissa, 2022).

Both Tanzania geodetic network and levelling network has several limitations which led to the development of the TAREF11 frame in 2010. TAREF11 (Tanzania Reference Frame of 2011), is a current geodetic network on which its computation has completed based on the “International Reference Frame of 2014 (ITRF14)” with January 1, 2011 as the reference epoch and because of that the new network has been named as Tanzania Reference Frame of 2011-TAREF11. TAREF11 is a three-dimensional modern geodetic reference network fully consistent and homogeneous with the International Terrestrial Reference Systems (ITRS). This frame consists of permanent and continuous GPS observing stations and it's the fundamental basis for the national and regional homogenous mapping supporting both post-mission and real time applications. TAREF11 comprises of 6 continuous observation reference stations (CORS), 16 zero order points, 72 first order points, and 504 second order point.

2.2 Physical Height System

These are height systems based on the earth's gravity field particularly determined using geodetic levelling technique that measure the distance between two equipotential surface of the earth's gravity field and provide height along the curved plumb line. The physical height system is referred to the geoid which is the most common used reference surface for establishment of the vertical datum. From the definition geoid, is an equal-potential surface of the earth's gravity field that approximately coincide with the MSL in a least square sense.

The traditional way to obtain physical heights is geodetic levelling in combination with gravity reductions along the so-called vertical or levelling networks. The gravity reductions are necessary to take into account the non-constant separation between equipotential surfaces due to variations of the Earth's gravity field. Depending on the gravity correction applied to levelling, different types of physical heights are distinguished: orthometric heights system, normal heights system, dynamic heights system and geopotential number.

2.2.1 Geopotential number (c)

The determination of the changes in the Earth's gravitational potential energy with respect to the potential of the geoid W_0 at points on or above the topography is what physical geodesy seeks for defining a level surface in space. Knowing the potential difference between two points involves the integral of gravity along a path between the two points (Bedada, 2010). A geopotential number is the difference between the Earth's gravity potential at the point of interest W and that on the

reference geopotential surface chosen W_0 (Hofmann-wellenhoff & Moritz, 2005). The geopotential number is measured in $\text{kgal}\cdot\text{m}$ and C is equal in the same equipotential surface. Although it has no distance dimension, it is the natural criterion for heights.

For a point on the surface of the earth, the geopotential number can be obtained by simply finding the difference between the potential on the geoid and that on the equal potential surface on which the point lies on the surface of the earth. Fluid flows from points with higher potential energy to points with lower potential energy. As the fluid flows the potential energy is converted to kinetic energy. Therefore, geopotential numbers Govern fluid flow hence becoming the physically meaningful and conceptually sensible height. Thus, spirit levelling height difference data needs to be corrected for gravity to reduce inconsistency that may cause levelling loop to have misclosures. See figure (2.1) below;

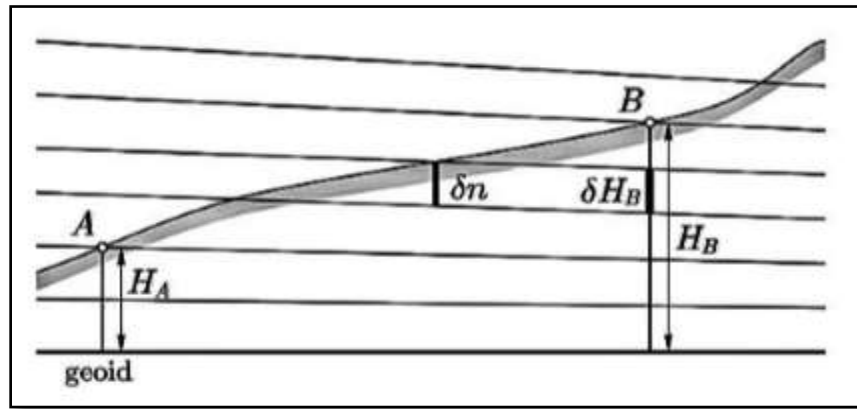


Figure 2.1: levelling and orthometric height (Hofmann-Wellenhof & Helmut, 2005)

Geopotential numbers have some cons to be used in physical applications, for example they have dimensions of length squared divided by time squared. The conversion of these dimensions is done by dividing the geopotential number by the value of gravity resulting to dimension of length. This process yields to another height system (dynamic, normal and orthometric).

Mathematically;

$$C = (W_0^{\text{LVD, TZG17}}) - W_p^{\text{GGM}} \dots\dots\dots (2.1)$$

where, C is geopotential number, $(W_0^{\text{LVD, TZG17}})$ is the actual potential on the reference surface (MSL) and W_p^{GGM} is the actual potential on the surface of the earth as obtained from XGM2019e

of maximum degree and order of 5540. Vertical Datum ($W_0^{\text{LVD, TZG13}}$) for Tanzania was initially calculated in 2016 and found to be $62636863.3242\text{m}^2/\text{s}^2$ (Masunga & Ulotu, 2016). This value was obtained from TZG13 Gravimetric Geoid Model and GPS & Ocean Levelling.

But in 2018 there was an update of geoid for Tanzania to form TZG17 with a better accuracy (5cm) than the 10cm-TZG13 by Peter, (2018). And in July 2015, the International Association of Geodesy (IAG) released a new conventional value of W_0 ($62636853.4\text{m}^2/\text{s}^2$) to define the global equipotential reference surface. Thus, by using these updated values Kamugisha, (2019) come up with an update of Tanzania Local Geopotential Vertical Datum from ($W_0^{\text{LVD, TZG13}}$) to ($W_0^{\text{LVD, TZG17}}$) at Tanga Tide Gauge Benchmark using GPS Levelling and TZG17 Geoid Model and the calculated value ($W_0^{\text{LVD, TZG17}}$) was found to be $62636852.42\text{m}^2/\text{s}^2$. Potential of gravity (W_p^{GGM}) on the surface of the earth for each point of the TAREF11 is obtained using the potential of gravitation (V) from spherical approximation equation and the centrifugal potential (Z).

2.2.2 Orthometric height

This is the length of the plumb line as measured from the geoid to the point on the surface of the earth. The orthometric height is given by the geopotential number divided by the integral mean value of gravity taken along the plumb line. Orthometric height has a clearer geometrical interpretation. The geoid reference surface is also unique, being the single equipotential surface of the Earth's gravity field that broadly corresponds with mean sea level in the open oceans (Featherstone & Kuhn, 2006). Figure (2.2) shows Orthometric height (H^0) as measured from the local geoid with a constant potential (W_0);

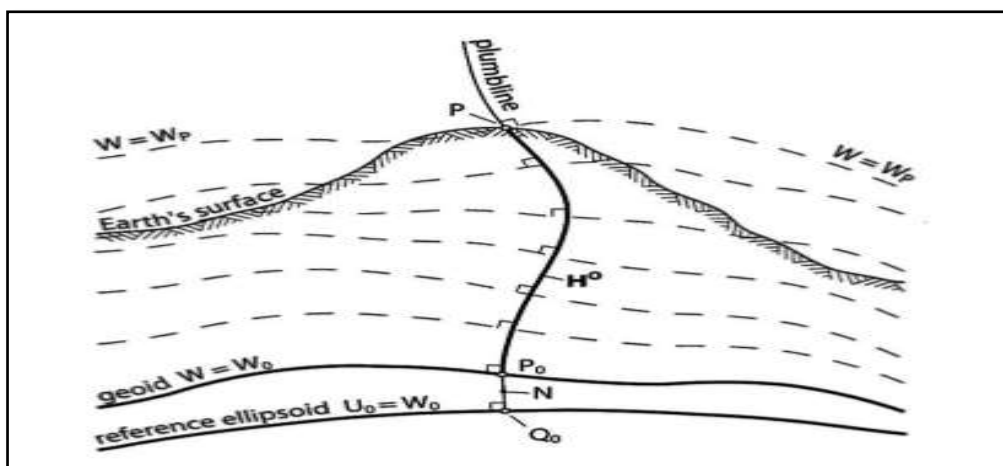


Figure 2.2: Definition of Orthometric height (Featherstone & Kuhn, 2006)

Mathematically; Orthometric height can be represented as;

$$H^o = \frac{C}{g_m} \dots\dots\dots (2.2)$$

Whereas C is the geopotential number and g_m is the mean gravity along the plumbline between the measured point and geoid.

It's difficult to measure directly orthometric height due to the fact that it requires knowledge inside the earth's surface. Thus, different approaches have been made to realize the orthometric heights. First approach involves the use of normal gravity so as to obtain so called normal orthometric height. In this approach geopotential number is replaced by spheropotential number and actual gravity is replaced by normal gravity. Advantage of this approach is that it involves avoidance of making gravity observations, but this is at the expense of losing information of the real Earth's gravity field. Another advantage is that only latitudes are needed along the levelling line. Normal orthometric height is obtained by the normal geopotential (spheropotential) number divided by the integral-mean value of normal gravity taken along the normal plumb line between the quasi-geoid and the point of interest (Idrissa, 2022).

Distinction from the normal height, where the integral mean normal gravity is taken between the ellipsoid and telluroid and the spheropotential number replaces the geopotential number.

$$H^{N-O} = \frac{C'}{\gamma} \dots\dots\dots (2.3)$$

Where H^{N-O} is Normal orthometric height, C' is Spheropotential number, γ is Normal gravity. Normal orthometric heights are easy to be computed but since they do not use surface gravity there are less likely to predict the fluid flow correctly.

On the other hand, another approach is based on the Poincare–Prey relationship for mean gravity and the Bouguer shell gravity expression that accounts for the topographic mass above the geoid but neglects the terrain effects. Therefore, the adopted mean gravity (\bar{g}) becomes (Heiskanen and Moritz, 1967).

$$\bar{g} = g^s + \frac{1}{2} FH - 2\pi G\rho H \dots\dots\dots (2.4)$$

where g^s is Observed Gravity at the topographic Surface, F is Free-air gravity gradient, G is Universal gravitational constant, ρ is topographic density, H is Spirit levelled height above MSL

Thus, the Helmert orthometric height can be obtained as follows from the above equation;

$$H^{H-O} = \frac{C}{g^s + \frac{1}{2}FH - 2\pi G\rho H} \dots\dots\dots (2.5)$$

Therefore, in order to compute Helmert orthometric height, the main input variables are geopotential number, surface point gravity, approximate height from MSL and crustal density.

2.2.3 Normal height

As different scientists faced the problem of determining the integral-mean value of actual gravity along the plumb line, then in 1945 Molodensky introduced the concept of the normal height system (Molodensky et al. 1962). The key differences from the orthometric height system are: the avoidance of hypotheses to determine the gravity field inside the topography; the theoretical replacement of the Earth's surface by the telluroid; and the use of a reference ellipsoid with associated gravity field (Torge, 2001). The telluroid is an auxiliary surface obtained by the pointwise projection of points P on the Earth's surface along the straight-line ellipsoidal normal to points Q that have the same gravity potential value in the normal gravity field U_Q as the original points P in the Earth's gravity field W_P , i.e., ($U_Q = W_P$) (See Figure 2-3).

As such, the telluroid is not an equipotential surface. The normal gravity field U approximates the real Earth's gravity field W and conceptually generated by masses within a reference ellipsoid (Moritz, 1992). Furthermore, Normal gravity can be calculated at any point without hypothesis and the normal gravity behaviour is very linear. Figure (2.3) shows the normal height and normal orthometric height as they are measure from quasi-geoid and geoid respectively.

Mathematically; Normal height from geopotential number can be represented as;

$$H^N = \frac{C}{\bar{\gamma}} \dots\dots\dots (2.6)$$

Whereas C is the geopotential number $\bar{\gamma}$ is Mean value of gravity taken along the plumb line.

Also, Normal height can be computed using height anomalies extracted from a quasi geoid. Mathematically normal height from height anomalies can be computed as;

$$H^N = h^{elp} - \zeta \dots\dots\dots (2.7)$$

Where h^{elp} is the ellipsoidal height of point on the topography obtained through GNSS positioning and ζ is the height anomaly computed by using quasi-geoid model.

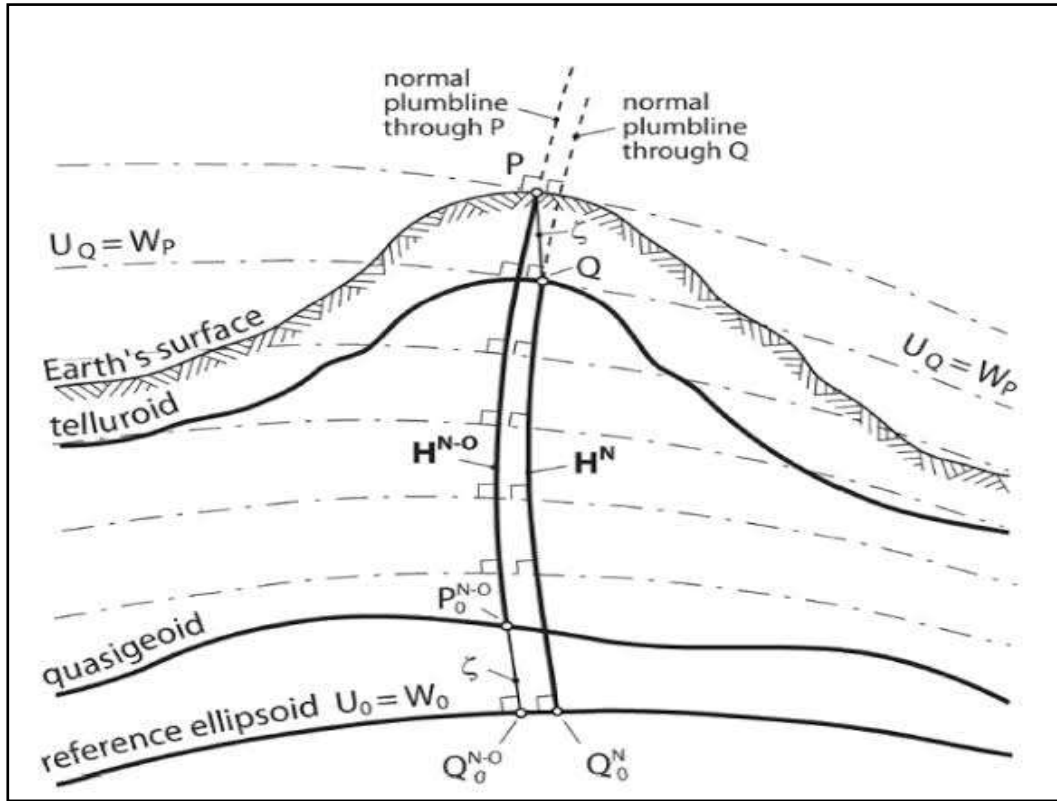


Figure 2.3: Normal orthometric height and normal height (Featherstone & Kuhn, 2006)

2.2.4 Dynamic height

Dynamic heights are just geopotential numbers, scaled into a metric unit. This system is most closely related to the system of geopotential numbers. Prior to the introduction of the geopotential number, the 8 dynamic height system proposed by Helmert (1884) was in use. Dynamic height is obtained by dividing the geopotential number by a constant normal gravity value (Heiskanen and Moritz, 1967). A gravity value at mid-latitude ($\pm 45^\circ$) has been taken as the global value, such as that generated by the reference ellipsoid.

Since the geopotential number is divided by a constant value, dynamic heights retain the same characteristics except that they have the dimension of length. Importantly, the flow of fluids is guaranteed from a greater to a lower height, and the theoretical loop closure is zero regardless of the chosen path. Due to its sensitiveness to fluid flow its used in some residual sets of tasks, mostly related to hydrodynamics and energetics of transporting mass such as construction of canals, dams and pipeline still requires geopotential height to map level surfaces on or above the Earth's surface.

Mathematically; Dynamic height can be represented as;

$$H_P^D = \frac{C_P}{\gamma_0} \dots\dots\dots (2.8)$$

Whereas C_P is the geopotential number and γ_0 is the constant normal gravity value, usually γ is 45°.

2.3 Overview of Global Geopotential Models (GGMs)

Global Geopotential Model is set of spherical harmonic coefficients of the earth gravity potential of external type i.e. external to the MES as the bounding surface (Ulotu, 2009). Global geopotential models are used to approximate the Earth's gravity potential and its functional. The GGMs are classified into two groups: models derived only from satellite missions, as well as models derived from satellite data integrated with terrestrial, satellite altimetry, airborne gravimetry, and topography/bathymetry data. The need of GGM originated upon the launch of the artificial satellite as early as in 1957, specifically the launch of the first laser tracked satellite, Beacon-B, in 1964, has provided datasets which have allowed researchers to determine long to medium components of the gravitational field of the Earth. In particular, observational data recorded at satellite laser ranging tracking 4 stations have since been used to develop the GGMs that quantify the global long wavelength and medium wavelength components of gravity field of the Earth (Lwehumbiza, 2017).

Recently many organizations and research centers have developed multi-Global Geopotential Models (GGMs) depending on several types of available gravity and height datasets to estimate orthometric heights from GNSS measurements. These includes, XGM2016, XGM2019e which is published in three versions truncated to d/o 2,160, 5,540, and 760, EIGEN-6C4, GO_CONS_GCF_2_TIM_R6e, and EGM2008. Each of these GGMs has its own advantages, and

their accuracy differs according to the region. For the case of this research study XGM2019e_5540 and WGM12 will be used for computation of gravity and gravitational potential of TAREF11 control points.

2.4 XGM2019e

XGM2019e is a combined global gravity field model represented by spheroidal harmonics up to degree and order (d/o) 5399, corresponding to a spatial resolution of 2' (~ 4 km). As data sources, it includes the satellite model GOCO06s in the longer wavelength range up to d/o 300 combined with a ground gravity grid which also covers the shorter wavelengths. The combination of the satellite data with the ground gravity observations is performed by using full normal equations up to d/o 719 (15'). Beyond d/o 719, a block-diagonal least squares solution is calculated for the high-resolution ground gravity data (from topography and altimetry). All calculations are performed in the spheroidal harmonic domain. The calculation of the XGM2019 spheroidal harmonic model coefficients up to d/o 719 consists of a weighted least squares adjustment of GOCO06s with the primary 15' NGA ground gravity dataset. All calculations are performed in the spheroidal harmonic domain. XGM19a is obtained by using the same LSA approach as for XGM2019 by combining GOCO06s and ground, but assigning an equal error of 2 mGal to all observations of the ground gravity grid (Zingerle et al., 2020).

2.5 WGM12

WGM2012 is the first release of a high-resolution grids and maps of the Earth's gravity anomalies (Bouguer, isostatic and surface free-air), computed at global scale in spherical geometry that take into account a realistic Earth model. It has been realized by the Bureau Gravimétrique International (BGI) in the frame of collaborations with international organizations such as Commission for the Geological Map of the World (CGMW), UNESCO, IAG, IUGG, International Union of Geological Sciences (IUGS) and with various scientific institutions.

WGM2012 gravity anomalies are derived from the available Earth global gravity models EGM2008 and DTU10 and include 1'x1' resolution terrain corrections derived from ETOPO1 model that consider the contribution of most surface masses (atmosphere, land, oceans, inland seas, lakes, ice caps and ice shelves). These products have been computed by means of a spherical harmonic approach using theoretical developments carried out to achieve accurate computations

at global scale (Balmino et al., 2011). Figure (2.4) shows a complete Bouguer gravity anomaly over Tanzania mainland surface.

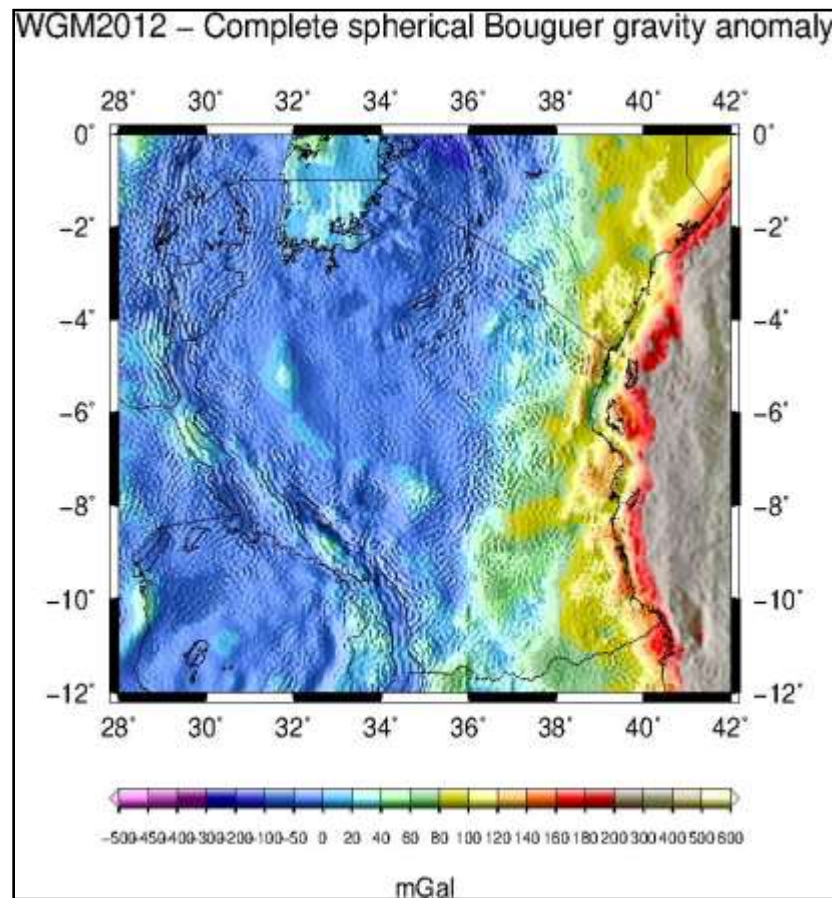


Figure 2.4: Complete Bouguer gravity anomaly over Tanzania mainland surface

2.6 Overview of Geoid and Quasi-geoid

The Geoid is defined as the equipotential surface of the Earth's gravity field which coincides with the sea surface in the absence of disturbing factors like tsunamis, ocean currents, salinities, wind and it extends through the continents (Vaníček & Krakiwsky, 1986). The geoid undulation N is the separation between the ellipsoid and the geoid measured along the ellipsoidal normal.

It is well known that rigorous determination of the geoid requires knowledge of the mass distribution of topography above the geoid. To avoid this problem (Molodensky et al., 1962) formulated the geodetic boundary value problem on the earth surface and introduced two new surfaces called the telluroid and the quasi-geoid, in which the geoidal undulation is replaced by height anomaly (Sadiq, 2009).

The quasi-geoid is a surface which fits best the mean sea level and coincide with the geoid in the oceans and continues under the Earth's surface. In difference to the geoid, the quasi-geoid is not an equipotential surface (gravity vector is not perpendicular to it). The height anomaly is the distance along the normal plumb line between the Earth's surface and the telluroid or between the ellipsoid and the quasi-geoid. (Sanchez, 2013).

The separation between the reference ellipsoid and the quasi-geoid is called the height anomaly and is defined as;

$$\zeta = h^{elp} - H^N \dots\dots\dots (2.9)$$

The telluroid is the surface defined by plotting the points at a distance equal to ζ below the earth surface. Figure 2.5 below shows the relationship of the geoid, quasigeoid and the reference ellipsoid

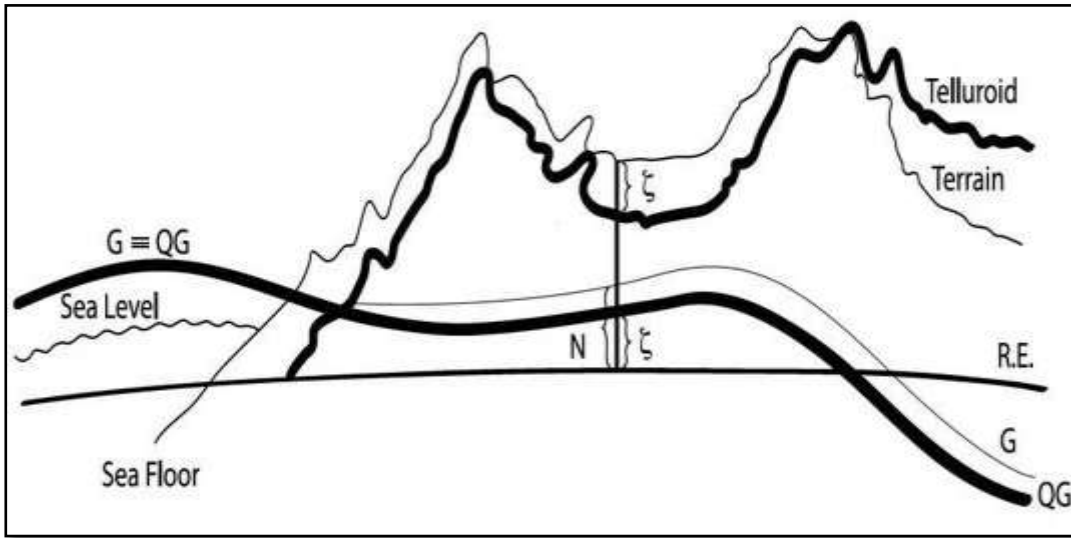


Figure 2.5: Relationship of the Quasi-geoid, geoid and the reference ellipsoid (Peter, 2018).

where G is Geoid, G.R.E. is Geodetic Reference Ellipsoid and QG is Quasi-geoid

2.6.1 A strict formula for Quasigeoid-Geoid separation (N- ζ)

Following (Heiskanen & Moritz, 1967), and (Hoffman & Moritz, 2006), the height anomaly ζ and geoid undulation N are related by;

$$N - \zeta = H^N - H = \frac{\bar{g} - \bar{\gamma}}{\bar{\gamma}} H \dots\dots\dots (2.10)$$

Where H is the orthometric height, H^N is the normal height whereas \bar{g} and $\bar{\gamma}$ are the mean gravity between the geoid and Earth's surface and mean normal gravity between the reference ellipsoid and telluroid, respectively (Ssegendo, 2015). The term $(\bar{g} - \bar{\gamma})$ is not directly available (Sjöberg, 2010) thus the geoid to quasi-geoid separation ($N - \zeta$) can be computed traditional by approximating it by the simple planar Bouguer gravity anomaly (Δg_B) at the computation point P (Heiskanen & Moritz, 1967). such that,

$$N - \zeta \approx \frac{\Delta g_P^B}{\gamma_0} H \dots\dots\dots (2.11)$$

Where $\bar{\gamma}$ in the denominator is replaced by the normal gravity for an arbitrary standard latitude (γ_0) usually 45° . Since long it is known that this formula is not accurate enough for precise height conversion in mountainous regions.

For a better approximation, (Flury & Rummel, 2009) added a so-called potential difference correction $[V_t(Q) - V_t(P)]\bar{\gamma}^{-1}$, where $V_t(Q)$ and $V_t(P)$ are the gravitational potential of the topographic masses (topographic potential) at the point P on the Earth's surface and Q on the geoid, respectively. For completeness, (Sjöberg, 2010) added the Gravity Gradient Correction $-\frac{H^2}{2\bar{\gamma}} \frac{\partial \Delta g_B}{\partial H}$. These corrections are accurate to the second order of the series expansion of the geoid to quasi-geoid separation (Sjöberg & Bagherbandi, 2017). The complete geoid to quasi-geoid separation in terms of the Bouguer anomaly read;

$$N - \zeta = \frac{\Delta g_P^B}{\gamma_0} H + \frac{V_t(Q) - V_t(P)}{\bar{\gamma}} - \frac{H^2}{2\bar{\gamma}} \frac{\partial \Delta g_B}{\partial H} \dots\dots\dots (2.12)$$

The topographic bias estimated to fourth powers of elevation according to spherical approximations and a constant density for topographic masses (Sjöberg, 2007) is given as:

$$\text{i.e.}; \quad \frac{V_t(Q) - V_t(P)}{\bar{\gamma}} = -\frac{2\pi\mu}{\bar{\gamma}} \left[H^2 + \frac{2}{3} \frac{H^3}{R} + \frac{n(n+1)}{12} \frac{H^4}{R} \right] \dots\dots\dots (2.13)$$

whereas, $\mu = G\rho$, G is the gravitational constant and ρ being the topographic density. Therefore; a strict formula for geoid to quasigeoid separation reads;

$$N - \zeta = \frac{\Delta g_P^B}{\gamma_0} H - \frac{2\pi\mu}{\bar{\gamma}} \left[H^2 + \frac{2}{3} \frac{H^3}{R} + \frac{n(n+1)}{12} \frac{H^4}{R} \right] - \frac{H^2}{2\bar{\gamma}} \frac{\partial \Delta g_B}{\partial H} \dots\dots\dots (2.14)$$

Whereas, $N - \zeta$, is the geoid to quasigeoid separation, Δg_B Bouguer gravity anomaly, H is the orthometric height and $\bar{\gamma}$ is the mean normal gravity.

CHAPTER THREE

METHODOLOGY

This part describes the techniques, methods, practical applications of different mathematical models, all data and the software used in this study to achieve the main objective of this research. It explains the procedures that will be implied in the computation of Dynamic and Orthometric heights and analysis of Normal heights for TAREF11 Controls Using TZQ17 quasi-geoid model, a strict formula, XGM 2019e_5540 Geopotential Model and World Gravity Model (WGM12).

3.1 Determination of the Actual Gravity Potential of TAREF11 controls

Actual gravity potential is a resultant of gravitational potential and centrifugal potential. Since geopotential numbers of all points are required for computation of normal, orthometric and dynamic height hence computation of gravity potential was needed. Gravitational potential can be expressed in terms of spherical harmonics as shown by equation (3.3). Equation (3.1) was used in computing actual gravity potential on the surface of the earth.

$$W_P = W_{(\gamma, \theta, \lambda)} = V_{(\gamma, \theta, \lambda)} + Z_{(\gamma, \theta, \lambda)} \dots\dots\dots (3.1)$$

Where $W_{(\gamma, \theta, \lambda)}$ is a potential of a point on the surface of the Earth, $Z_{(\gamma, \theta, \lambda)}$ is centrifugal potential given by equation (3.2) and $V_{(\gamma, \theta, \lambda)}$ is a Gravitational potential given by equation (3.3).

$$Z_{(r, \theta)} = \frac{W^2}{2} r^2 (\sin \theta)^2 \dots\dots\dots (3.2)$$

Where, W is earth's rotation rate, θ is co-latitude, r is radial distance and $Z_{(r, \theta)}$ is centrifugal potential. Also;

$$V_{(r, \theta, \lambda)} = \frac{GM}{R} \sum_{n=0}^{\infty} \sum_{m=0}^n \left(\frac{R}{r}\right)^{(n+1)} C_{nm} Y_{nm}(\theta, \lambda) \dots\dots\dots (3.3)$$

where λ is Longitude, GM is Product of mass of the earth and Newton's gravitational constant, R is Mean earth radius, C_{nm} is constant coefficient for degree n and order m , Y_{nm} is fully normalized equation of surface spherical harmonic function given by equation (3.4).

$$Y_{nm} = \begin{cases} P_{nm}(\cos\theta)\cos|m|\lambda, m \geq 0 \\ P_{n|m|}(\cos\theta)\sin|m|\lambda, m < 0 \end{cases} \dots\dots\dots (3.4)$$

Where P_{nm} are fully normalized Legendre. The spherical harmonics coefficients are to be obtained from XGM2019e having maximum degree and order of 5540. Thus, by using the inputs from equation (3.2) and equation (3.3) and plug those in equation (3.1) actual gravity potential can be determined. All these mathematical equations have been programmed in the GrafLab for simplification of computation of the actual gravity potential. Graf lab user interface as used in computation of gravity and gravity potential is shown in the Figure (3.1).

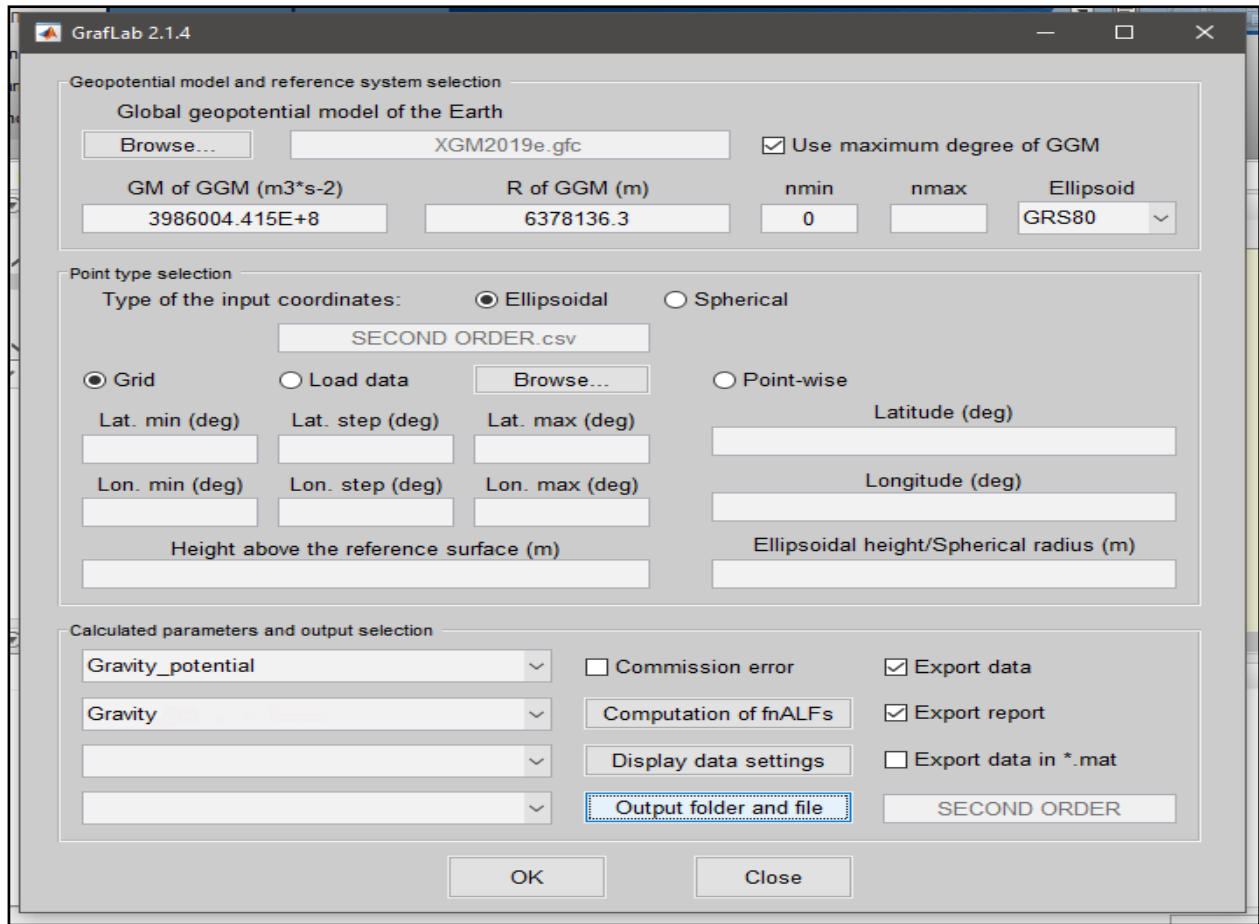


Figure 3.1: A GUI of Graf lab software that was used in computations of actual gravity potential on the surface of the earth.

From Figure (3.1), the GUI has three main sections, the first section deals with selection of GGM. In case of this study XGM2019e_5540(d/o) downloaded from ICGEM website (<http://icgem.gfz->

potsdam.de/tom_longtime) was used. In the same section for computations of actual gravity potential and surface gravity minimum degree (nmin) was set to zero and maximum degree (nmax) was set as specified by selected GGM (5540). The second section is point type selection, where by ellipsoidal coordinates of the TAREF11 control points were imported. The last section is calculated parameters and output selection sections where by output folder and required output parameters W_p^{GGM} and surface gravity were set. Finally, actual gravity potential and surface gravity of the selected points on the surface of the earth were computed as shown in Figure (3.2).

Software 2.1.4 (GUI used) Computer name DESKTOP-1IHM3TF
Generating date 18-Apr-2023 Generating time 18:26:47 MATLAB version
9.0.0.341360 (R2016a) Computed Functionals of the geopotential Imported

data file D:\TAREF11\CORZERO.csv Geopotential model file D:
TAREF11\XGM2019e.gfcGM of the geopotential model (m^3*s^{-2}) 3.98600441500000e+14R of the geopotential model (m)
6.3781363000000e+06Minimum used degree 0Maximum used degree 5540Reference
ellipsoid GRS80Type of the input coordinates EllipsoidLatitude limit North (deg)
-1.3255469390000e+00Latitude limit South (deg) -1.1273672910000e+01Longitude limit West (deg)
2.9668363250000e+01Longitude limit East (deg) 4.0184943690000e+01Number of points
18Computation time (dd:hh:mm:ss) 00:00:01:31Computation of fully normalized ALFs Standard
forward column methodExported data file contains the following columns:Ellipsoid Latitude (deg) Longitude (deg) Height above the reference
ellipsoid (m) Gravity (mGal) Gravity_potential (m^2*s^{-2}) Gravity_disturbance (mGal) Disturbing_potential (m^2*s^{-2})

-5.040146003000e+00	3.282545506000e+01	1.204850100000e+03	9.776600706711e+05	6.262489563811e+07	-4.036690934299e+01	-1.831448717360e+02
3.349947100000e+00	3.733710299000e+01	8.406029000000e+02	9.777592301329e+05	6.262845619428e+07	-3.145871324541e+01	-1.842273163676e+02
6.765585222000e+00	3.920792563000e+01	7.046070000000e+01	9.780741121009e+05	6.263589697219e+07	-8.187178412378e+00	-2.747063617050e+02
6.817814342000e+00	3.929718149000e+01	2.239570000000e+01	9.780909994912e+05	6.263636468498e+07	-7.242765882154e+00	-2.771122832783e+02
6.218534344000e+00	3.921071639000e+01	-3.975800000000e+00	9.780787836502e+05	6.263661983257e+07	-1.544496209451e+01	-2.799045370628e+02
6.169643667000e+00	3.574830403000e+01	1.099970500000e+03	9.777394174869e+05	6.262590445213e+07	-1.309245762897e+01	-1.995386487833e+02
1.127367291000e+01	3.480027731000e+01	5.233506000000e+02	9.780073145041e+05	6.263155659070e+07	-6.026589253878e+01	-1.851093934659e+02
1.106259767000e+01	3.734052871000e+01	6.728775000000e+02	9.779927390185e+05	6.263005408149e+07	-2.157420607940e+01	-2.252263173049e+02
1.033472591000e+01	4.018494369000e+01	8.681930000000e+01	9.781898811491e+05	6.263576074445e+07	1.845028492617e+01	-2.508518260504e+02
7.675926314000e+00	3.575315665000e+01	1.411340400000e+03	9.777187986761e+05	6.262288415955e+07	2.998263879661e+01	-1.750945569693e+02
7.951186911000e+00	3.160571506000e+01	1.791212700000e+03	9.776862941912e+05	6.261923328673e+07	1.000363648319e+02	-1.120999928052e+02
5.087755350000e+00	3.911662974000e+01	-1.593710000000e+01	9.780303038106e+05	6.263673922768e+07	-4.770137710555e+01	-2.774992770413e+02
5.040230144000e+00	3.282546330000e+01	1.201499000000e+03	9.776611054937e+05	6.262492839267e+07	-4.036731629213e+01	-1.831462179573e+02
4.806717589000e+00	2.966836325000e+01	8.080352000000e+02	9.777641738521e+05	6.262879923909e+07	-5.634129062830e+01	-1.594678125337e+02
1.325546939000e+00	3.179922476000e+01	1.237596400000e+03	9.77640084506e+05	6.262460841157e+07	-1.329530949921e+01	-1.506713266374e+02
2.446997372000e+00	3.292251841000e+01	1.127871300000e+03	9.776721382532e+05	6.262565767039e+07	-2.174000895312e+01	-1.740872646219e+02
1.537530333000e+00	3.383794936000e+01	1.167988700000e+03	9.776468488525e+05	6.262526272956e+07	-2.890033485081e+01	-1.768717172454e+02
6.748471417000e+00	3.780492904000e+01	4.803136000000e+02	9.779433759075e+05	6.263193270256e+07	-1.201355606852e+01	-2.305372056179e+02

Figure 3.2: Sample of extracted Gravity and Gravity potential data from XGM2019e_5540 GGM.

3.2 Determination of the Geopotential Number

By using actual gravity potential (W_p) on the surface of the earth as computed using Combined Global Geopotential Model (XGM2019e) with maximum degree of 5540 as explained in Sect 3.1

and local geopotential vertical datum ($W_0^{LVD, TZG17}$) having the value of $62636852.42m^2/s^2$ computed by (Kamugisha, 2019) which was computed using GPS-levelling and TZG17 gravimetric geoid model. Geopotential number in this research was obtained using equation (2.1).

3.3 Extraction of height anomaly (ζ_p) from TZQ17 quasi-geoid

The height anomalies values of each coordinated TAREF11 control were obtained by interpolation (sampling of a point) method using the GPS/levelling data i.e. (ϕ, λ). The geographical coordinates of a specific points (ϕ, λ) were used to get height anomaly of the respective points $\zeta_p(\phi, \lambda)$.

Where by the gridded file of TZQ17 quasi-geoid covering the area of interest was loaded into golden surfer software and the TAREF11 geographical coordinates (ϕ, λ) was added to see their distribution over the quasi-geoid surface.

Then, height anomalies were extracted by importing gridded file of quasi-geoid and the geographical coordinates file in csv formats. Thereafter the grids values (height anomalies) were extracted. Figure (3.3) shows the inputs and the output for extractions of height anomalies.

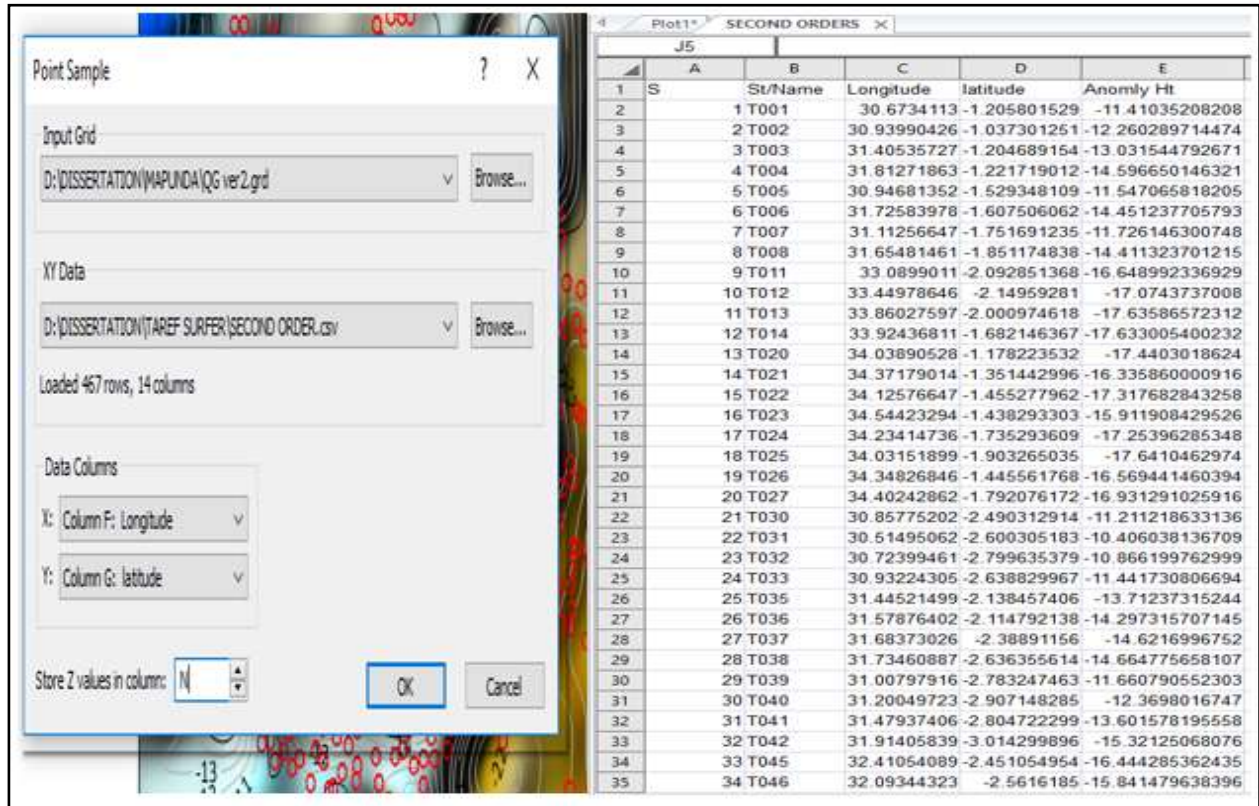


Figure 3.3: Inputs and output section for extraction of height anomalies

3.4 Extraction of geoid undulation(N) from TZG17 geoid model

The geoid undulation values of each coordinated TAREF11 control was obtained by interpolation (sampling of a point) method using the GPS/levelling data i.e. (ϕ, λ) . The geographical coordinates of a specific points (ϕ, λ) were used to get geoid undulation of the respective points $N_p(\phi, \lambda)$. Extraction of geoid undulation was done by importing TZG17 gridded file along with geographical coordinates file in csv formats and then the geoid undulation grided values was extracted. Figure (3-4) shows the inputs and the output for extractions of geoid undulation.

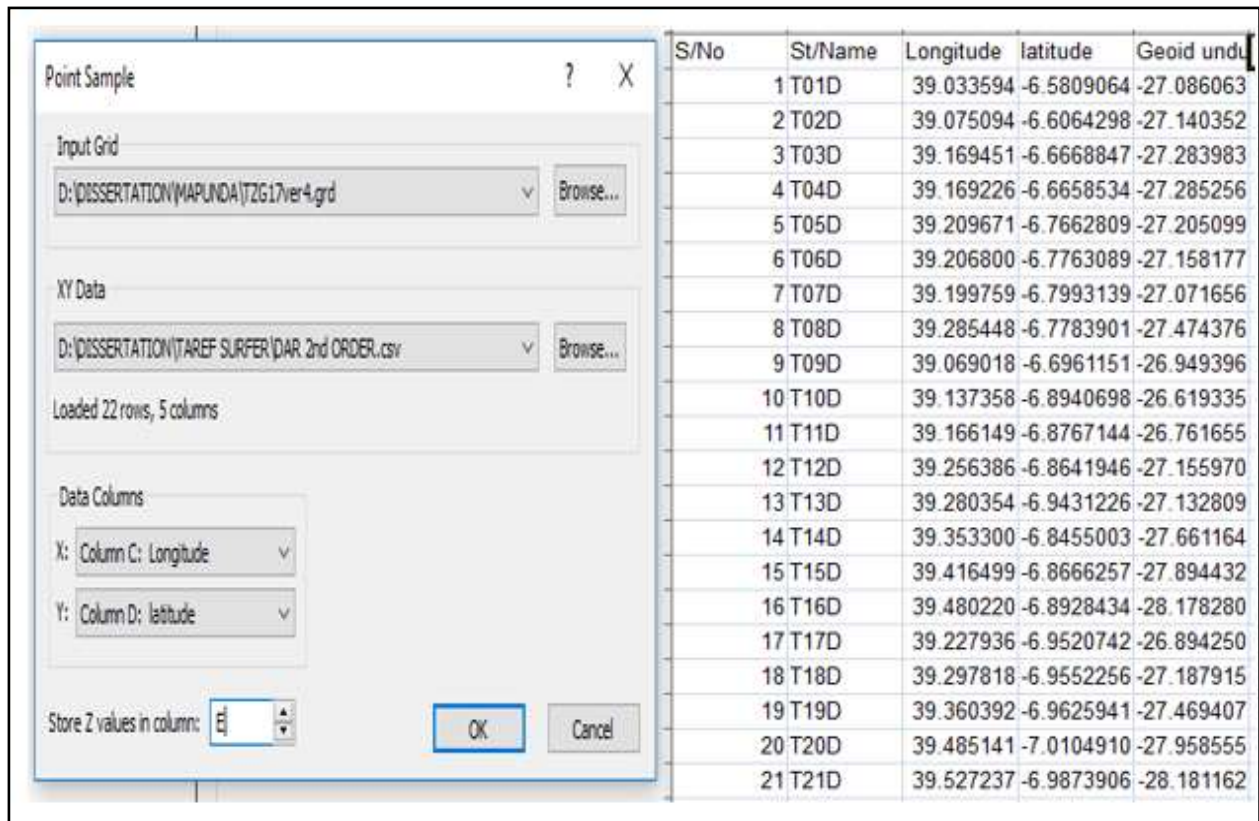


Figure 3.4: Inputs and output section for extraction of geoid undulation

3.5 Computation of Normal Gravity

The normal gravity on telluroid and GRS80 were computed using Equation 3.5 and 3.6 from (Moritz, 1980).

$$\gamma_Q = [\gamma_0 - (0.3087691 - 0.0004398 \sin^2 \varphi)h_Q + 7.2125 \times 10^{-8} h_Q^2] mgal \dots\dots\dots (3.5)$$

$$\gamma_0^{GRS80} = [978032.7(1 + 0.0053024 \sin^2 \varphi - 0.0000058 \sin^2 2\varphi)] mgal \dots\dots\dots (3.6)$$

Where γ_0^{GRS80} is the normal gravity on reference ellipsoid (GRS80), φ is geographical coordinate and h_Q Is the normal height on telluroid above a reference ellipsoid given by equation 2.7 .

After determination of height anomaly and ellipsoid height from quasi-geoid and GPS positioning respectively, normal height was computed using equation 3.7 and hence the normal gravity on telluroid using equation (3.6).

3.6 Computation of mean normal gravity

After the determination of normal gravity on telluroid, the mean normal gravity was then computed. The mean normal gravity was computed by using equation 3.8.

$$\bar{\gamma} = \gamma_0 - 0.1543H(mgal/m) \dots\dots\dots (3.8)$$

Where $\bar{\gamma}$ is the mean normal gravity along the plumb line between point and quasi geoid, γ_0 is the normal gravity and H is the height in meter.

3.7 Computation of mean gravity

After the determination of surface gravity from XGM2019e_5540 degree and order using the Graflab user interface, the mean gravity was then computed. The mean gravity was computed by Poincare-Prey reduction formula as;

$$\bar{g} = g_p + 0.0424H(gal / km) \dots\dots\dots (3.9)$$

Where \bar{g} is the mean gravity along the plumb line between point and geoid, g_p is the point surface gravity and H is the levelling height in kilometers.

3.8 Computation of Normal Heights Using Geopotential Numbers

After the computation of geopotential number and mean normal gravity, the normal height is computed using the equation (2.6) which is called normal height by fundamental approach (Heiskanen & Moritz, 1967).

3.9 Computation of Normal Heights Using TZQ 17 quasi-geoid

After the extraction of height anomaly from quasi-geoid and the available ellipsoidal height of the TAREF11 controls, the normal height was computed using the equation (2.7). Where the inputs

were ellipsoidal height of point on the topography obtained through GNSS positioning and the height anomaly computed by using TZQ17 quasi-geoid model.

3.10 Computation of Normal height by a strict formula

Normal height by a strict formula was computed by first computing the geoid to quasi-geoid separation and then computation of height anomalies from the computed geoid to quasi-geoid separation values. Geoid to Quasi-geoid separation was computed using equation (2.14).

In this study WGM12 Bouguer gravity anomalies data downloaded from BGI website (<https://bgi.obs-mip.fr/data-products/outils/wgm2012-maps-visualizationextraction/>) are used. The downloaded WGM12 complete Bouguer gravity anomaly gridded file is then imported in Golden surfer software along with geographical coordinates file in csv formats and then the Bouguer gravity anomalies values of TAREF11 controls points were extracted. Figure (3-5) shows the inputs and the output for extractions of Bouguer gravity anomalies.

Point Sample					S/No	St/Name	Longitude	latitude	BougWGM12
Input Grid					1	ARIT	32.825455	-5.0401460	-44.97749221
D:\DISSERTATION\TAREF SURFER\ALOSDEM\...\WGM2012.grd					2	MOSH	37.337103	-3.3499471	-9.016032029
Browse...					3	TANZ	39.207926	-6.7655852	129.35971344
XY Data					4	DARA	39.297181	-6.8178143	128.86512025
D:\DISSERTATION\TAREF SURF... \CORS & ZERO ORDER .csv					5	ZNZB	39.210716	-6.2185343	121.65213156
Browse...					6	DODC	35.748304	-6.1696437	-12.28613455
Loaded 19 rows, 15 columns:					7	T01Z	34.800277	-11.273673	11.094549637
Data Columns					8	T02Z	37.340529	-11.062598	44.636683754
X: Column F: Longitude					9	T03Z	40.184944	-10.334726	155.20101691
Y: Column G: latitude					10	T05Z	35.753157	-7.6759263	-13.74195675
Store 2 values in column: E					11	T07Z	31.605715	-7.9511869	2.3172520231
OK Cancel					12	T09Z	39.116630	-5.0877554	94.349999919
					13	T11Z	32.825463	-5.0402301	-44.97790036
					14	T12Z	29.668363	-4.8867176	-17.86832050
					15	T13Z	31.799225	-1.3255469	-24.57101531
					16	T14Z	32.922518	-2.4469974	-16.99143576
					17	T15Z	33.837949	-1.5375303	-41.65091263
					18	T16Z	37.804929	-6.7484714	75.656034078

Figure 3.5: Inputs and output section for extraction of Bouguer gravity anomalies

After extraction of Bouguer gravity anomalies from WGM12 along with topographic correction, gravity gradient corrections, orthometric heights as well as computed normal gravity and mean

normal gravity then $N - \zeta$ (geoid to quasi-geoid separation) values were computed using the equation 2.14. After computation of $N - \zeta$ value, the height anomalies of all TAREF11 controls were then computed and later on computation of Normal height using equation 2.7.

3.11 Computation of Orthometric height from geopotential number

After the computation of mean gravity of TAREF11 controls and available geopotential number then the Orthometric height was computed using equation (2.2). Where the inputs were the geopotential number computed using XGM2019e_5540 d/o, and the mean gravity (g_m) along the actual plumbline between the measured point and geoid.

3.12 Computation of Orthometric height from TZG17

After the extraction of geoid undulation from TZG17 geoid model and the available ellipsoidal height of the TAREF11 controls, the Orthometric height was computed using the formula below as;

Mathematically; orthometric height from geoid model can be represented as;

$$H^{O(TZG17)} = h^{elp} - N^{TZG17} \dots\dots\dots (3.10)$$

Where h^{elp} is the ellipsoidal height of point on the topography obtained through GNSS positioning and N^{TZG17} is the geoid undulation extracted from TZG17 geoid model.

3.13 Computation of Dynamic height from geopotential number

After the computation of the constant normal gravity value (γ_o) of TAREF11 controls and available geopotential number then the dynamic height was computed using equation (2.8). Where the inputs were the geopotential number computed using XGM2019e_5540 d/o and the constant normal gravity value (γ_o), usually γ is 45° .

3.14 Data used and its sources

From equation (2.1 to 3.10) the key input parameters shows the nature and type of data that are important in completion of this study. Different data such as TAREF11 controls points coordinates, actual gravity potential (W_p^{GGM}), heights anomalies (ζ), geoidal undulation from TZG17, TZQ17, XGM2019e_5540 and Bouguer gravity anomalies from WGM12 have been used for completion of this research. All data that have been used in this research study are summarized in Table (3.1) with their associated reliable source.

Table 3.1: Data used in this research

DATA	SOURCES
GGM Data (XGM2019e_5540)	ICGEM (icgem.gfzportdam.de/tom_longtime).
TAREF11 control points coordinates	DGST
TZQ17 Quasi- geoid	DGST
TZG17 Geoid model	DGST
Heights Anomalies of TAREF11 controls.	TZQ17 Quasi- geoid
Bouguer Gravity anomaly data (WGM12)	BGI (https://bgi.obs-mip.fr/#)

i. XGM2019e_5540

It was used in computation of component of actual gravity potential for determination of Geopotential number as well as extraction of surface gravity for computation of mean gravity.

ii. WGM12

It was used in extraction of Bouguer gravity anomalies for determination of geoid to quasi-geoid separation.

iii. TAREF11 control points geographical coordinates

It was used in computation of normal gravity, mean normal gravity, and mean gravity and extraction of height anomalies (ζ).

iv. TZQ17 quasi-geoid

This is a source of height anomalies (ζ) for determination of the normal heights.

v. TZG17

This is a source of geoid undulation (N) for determination of the orthometric heights.

3.14.1 Software

In this research different software were installed and used for performing different tasks. These software were used for data computation, data processing, data analysis as well as report preparation and writing. All software have played a vital role in completion of this research. Table (3.2) shows all important software that was installed and used in this research.

Table 3.2: Software that was installed and its uses in this research.

Software Name	Use
Microsoft Excel	For data arrangement and in computation of different mathematical functions.
MATLAB	For computation of component of actual potential (W_p) on the surface of the Earth.
Graflab	Act as program to be used in MATLAB for computation of different gravity parameters.
Golden Surfer18	For extraction of heights anomalies, Geoid undulation, Bouguer gravity anomalies as well as statistical analysis of the results
Microsoft word	For report writing.
ARCGIS	For preparation of study area map

Graflab is MATLAB-based graphical user interface program for computing functional of the geopotential including actual gravity potential (W_p) and surface gravity (g_p) up to ultra-high degrees and orders. This program allows the computation of 38 functional of the geopotentials up to ultra-high degrees and orders of spherical harmonic expansion. The computation of the geopotential functions is done by applying the technique so called lumped coefficients approach (Bucha & Janak, 2013).

CHAPTER FOUR

RESULTS AND ANALYSIS

4.1 Results

This chapter present the results and discussion of the results obtained in this research. The outputs of this study are geopotential number, normal gravity, mean normal gravity, mean gravity, normal heights using geopotential number, TZQ17 quasigeoid model and strict formula, orthometric heights using geopotential number and TZG17 geoid model and dynamic heights using geopotential number.

4.1.1 Extracted surface gravity and actual gravity potential of TAREF11 control points

The surface gravity and actual gravity potential of TAREF11 controls points used in this study were computed using equation (3.1) by Graflab user interface as explained in sect. (3.1). Here under are the obtained results of the computed and extracted surface gravity and actual gravity potential as shown in Table 4.1

Table 4.1: Computed actual gravity potentials of TAREF11 Control points

S/No	St/Name	Zone	Order	Gravity (m/s^2)	Gravity Potential (Wp) (m^2/s^2)
1	ARIT	36s	CORS	9.776600707	62624895.64
2	MOSH	37s	CORS	9.777592301	62628456.19
3	TANZ	37s	CORS	9.780741121	62635896.97
4	DARA	37s	CORS	9.780909995	62636364.68
5	ZNZB	37s	CORS	9.780787837	62636619.83
6	DODC	36s	CORS	9.777394175	62625904.45
7	T01Z	36s	Zero	9.780073145	62631556.59
8	T02Z	37s	Zero	9.77992739	62630054.08
9	T03Z	37s	Zero	9.781898811	62635760.74
10	T05Z	36S	Zero	9.777187987	62622884.16
11	T07Z	36s	Zero	9.776862942	62619233.29
12	T09Z	37s	Zero	9.780303038	62636739.23
13	T11Z	36s	Zero	9.776611055	62624928.39
14	T12Z	35s	Zero	9.777641739	62628799.24
15	T13Z	36s	Zero	9.776400985	62624608.41
16	T14Z	36S	Zero	9.776721383	62625657.67

4.1.2 Computed Geopotential numbers of TAREF11 Control points

The geopotential number of each TAREF11 control points used in this study were computed using Equation (3.5) as explained in Sect. (3.2) and the here under are the obtained results of the computed actual gravity potential as shown in Table 4.2. Where, W_p is the actual gravity potential on the surface of the earth, W_0 is Local geopotential vertical datum ($W_0^{LVD, TZG17}$) and C_p is the geopotential number.

Table 4.2: Computed geopotential number values of TAREF11 Control points

S/No	St/Name	Zone	Order	W_p (m^2/s^2)	($W_0^{LVD, TZG17}$) (m^2/s^2)	C_p (m^2/s^2)
1	ARIT	36s	CORS	62624895.64	62636852.42	11956.781
2	MOSH	37s	CORS	62628456.19	62636852.42	8396.225
3	TANZ	37s	CORS	62635896.97	62636852.42	955.447
4	DARA	37s	CORS	62636364.68	62636852.42	487.735
5	ZNZB	37s	CORS	62636619.83	62636852.42	232.587
6	DODC	36s	CORS	62625904.45	62636852.42	10947.967
7	T01Z	36s	Zero	62631556.59	62636852.42	5295.829
8	T02Z	37s	Zero	62630054.08	62636852.42	6798.338
9	T03Z	37s	Zero	62635760.74	62636852.42	1091.675
10	T05Z	36S	Zero	62622884.16	62636852.42	13968.260
11	T07Z	36s	Zero	62619233.29	62636852.42	17619.133
12	T09Z	37s	Zero	62636739.23	62636852.42	113.192
13	T11Z	36s	Zero	62624928.39	62636852.42	11924.027
14	T12Z	35s	Zero	62628799.24	62636852.42	8053.180
15	T13Z	36s	Zero	62624608.41	62636852.42	12244.008
16	T14Z	36S	Zero	62625657.67	62636852.42	11194.749
17	T15Z	36S	Zero	62625262.73	62636852.42	11589.690
18	T16Z	37s	Zero	62631932.7	62636852.42	4919.717
19	T01F	36s	First	62620736.44	62636852.42	16115.975
20	T02F	36s	First	62621048.97	62636852.42	15803.445
21	T03F	36s	First	62619383.86	62636852.42	17468.558
22	T04F	36s	First	62622795.71	62636852.42	14056.706
23	T05F	36s	First	62622158.93	62636852.42	14693.494
24	T06F	36s	First	62617071.98	62636852.42	19780.441
25	T07F	36s	First	62623861.08	62636852.42	12991.342
26	T08F	36s	First	62622384.95	62636852.42	14467.466

4.1.3 Extracted height anomaly (ζ_p) of TAREF11 controls from TZQ17 quasi-geoid model

The height anomalies information was extracted from TZQ17 quasi-geoid model following all the steps as explained in sect (3.3) and the final results are presented in the Table 4.3 where, λ geographical longitude φ is the geographical latitude and ζ_p is the height anomaly.

Table 4.3: Extracted height anomaly (ζ_p) values of TAREF11 control points

S/No	St/Name	Zone	Order	λ (d.ddd)	φ (d.ddd)	ζ (meter)
1	ARIT	36s	CORS	32.82546	-5.040146	-17.524
2	MOSH	37s	CORS	37.3371	-3.349947	-16.993
3	TANZ	37s	CORS	39.20793	-6.765585	-27.052
4	DARA	37s	CORS	39.29718	-6.817814	-27.418
5	ZNZB	37s	CORS	39.21072	-6.218534	-28.484
6	DODC	36s	CORS	35.7483	-6.169644	-20.217
7	T01Z	36s	Zero	34.80028	-11.27367	-18.459
8	T02Z	37s	Zero	37.34053	-11.0626	-21.910
9	T03Z	37s	Zero	40.18494	-10.33473	-25.046
10	T05Z	36S	Zero	35.75316	-7.675926	-16.296
11	T07Z	36s	Zero	31.60572	-7.951187	-10.681
12	T09Z	37s	Zero	39.11663	-5.087755	-27.267
13	T11Z	36s	Zero	32.82546	-5.04023	-17.524
14	T12Z	35s	Zero	29.66836	-4.886718	-16.761
15	T13Z	36s	Zero	31.79922	-1.325547	-14.576
16	T14Z	36S	Zero	32.92252	-2.446997	-16.608
17	T15Z	36S	Zero	33.83795	-1.53753	-17.602
18	T16Z	37s	Zero	37.80493	-6.748471	-22.769
19	T01F	36s	First	31.15054	-1.531898	-11.979
20	T02F	36s	First	34.68163	-1.834966	-16.333
21	T03F	36s	First	30.66942	-2.506662	-10.723
22	T04F	36s	First	31.36577	-2.664347	-13.191
23	T05F	36s	First	34.81976	-2.436597	-15.954
24	T06F	36s	First	35.54513	-2.067269	-15.678
25	T07F	36s	First	36.7041	-2.742595	-16.165
26	T08F	36s	First	30.70853	-3.593106	-11.968
27	T09F	36s	First	31.52459	-3.335702	-13.979
28	T10F	36s	First	32.40739	-3.405327	-16.397
29	T11F	36s	First	33.40612	-3.370276	-18.307
30	T12F	36s	First	34.30568	-3.517024	-19.401

4.1.4 Extracted geoid undulation (N) of TAREF11 control points from TZG17 geoid model

The height anomalies information was extracted from TZG17 geoid model following all the steps as explained in sect (3.4) and the final results are presented in the Table 4.4 where, λ geographical longitude φ is the geographical latitude and N is the Geoid undulation.

Table 4.4: Extracted geoid undulation (N) values of TAREF11 controls from TZG17

S/No	St/Name	Zone	Order	λ (d.ddd)	φ (d.ddd)	N (meter)
1	ARIT	36s	CORS	32.82546	-5.040146	-18.044
2	MOSH	37s	CORS	37.3371	-3.349947	-17.752
3	TANZ	37s	CORS	39.20793	-6.765585	-27.201
4	DARA	37s	CORS	39.29718	-6.817814	-27.441
5	ZNZB	37s	CORS	39.21072	-6.218534	-27.696
6	DODC	36s	CORS	35.7483	-6.169644	-19.704
7	T01Z	36s	Zero	34.80028	-11.27367	-17.748
8	T02Z	37s	Zero	37.34053	-11.0626	-22.121
9	T03Z	37s	Zero	40.18494	-10.33473	-24.711
10	T05Z	36S	Zero	35.75316	-7.675926	-17.292
11	T07Z	36s	Zero	31.60572	-7.951187	-11.394
12	T09Z	37s	Zero	39.11663	-5.087755	-27.533
13	T11Z	36s	Zero	32.82546	-5.04023	-18.044
14	T12Z	35s	Zero	29.66836	-4.886718	-15.433
15	T13Z	36s	Zero	31.79922	-1.325547	-14.762
16	T14Z	36S	Zero	32.92252	-2.446997	-17.063
17	T15Z	36S	Zero	33.83795	-1.53753	-17.449
18	T16Z	37s	Zero	37.80493	-6.748471	-22.566
19	T01F	36s	First	31.15054	-1.531898	-12.559
20	T02F	36s	First	34.68163	-1.834966	-16.790
21	T03F	36s	First	30.66942	-2.506662	-10.853
22	T04F	36s	First	31.36577	-2.664347	-13.291
23	T05F	36s	First	34.81976	-2.436597	-16.564
24	T06F	36s	First	35.54513	-2.067269	-15.815
25	T07F	36s	First	36.7041	-2.742595	-16.607
26	T08F	36s	First	30.70853	-3.593106	-12.450
27	T09F	36s	First	31.52459	-3.335702	-14.218
28	T10F	36s	First	32.40739	-3.405327	-16.707
29	T11F	36s	First	33.40612	-3.370276	-18.506

4.1.5 Computed normal gravity of TAREF11 control points

The normal gravity on telluroid (γ_Q) information used in this study were computed using equation 3.5 in which key inputs were normal gravity (γ_O) on reference ellipsoid (GRS80) computed using equation 3.6, normal height (h_Q) and geographical coordinate φ as explained in sect (3.5) and the final results are in Table 4.5. Where, φ is the geographical latitude and γ_0^{GRS80} is normal gravity on GRS80 and γ_Q is normal gravity on telluroid.

Table 4.5: Computed normal gravity values of TAREF11 control points.

S/No	St/Name	Zone	Order	φ (d.ddd)	γ_0^{GRS80} (m/s^2)	γ_Q (m/s^2)
1	ARIT	36s	CORS	-5.040146	9.780726	9.77695233
2	MOSH	37s	CORS	-3.349947	9.780503	9.77785585
3	TANZ	37s	CORS	-6.765585	9.781044	9.78074255
4	DARA	37s	CORS	-6.817814	9.781055	9.78090087
5	ZNZB	37s	CORS	-6.218534	9.780933	9.78085718
6	DODC	36s	CORS	-6.169644	9.780923	9.77746557
7	T01Z	36s	Zero	-11.27367	9.782301	9.78062800
8	T02Z	37s	Zero	-11.0626	9.782228	9.78008350
9	T03Z	37s	Zero	-10.33473	9.781989	9.78164357
10	T05Z	36S	Zero	-7.675926	9.781248	9.77684171
11	T07Z	36s	Zero	-7.951187	9.781315	9.77575386
12	T09Z	37s	Zero	-5.087755	9.780733	9.78069808
13	T11Z	36s	Zero	-5.04023	9.780726	9.77696268
14	T12Z	35s	Zero	-4.886718	9.780702	9.77815548
15	T13Z	36s	Zero	-1.325547	9.780355	9.77648944
16	T14Z	36S	Zero	-2.446997	9.780421	9.77688827
17	T15Z	36S	Zero	-1.53753	9.780364	9.77670445
18	T16Z	37s	Zero	-6.748471	9.781040	9.77948687
19	T01F	36s	First	-1.531898	9.780364	9.77527805
20	T02F	36s	First	-1.834966	9.780380	9.77539172
21	T03F	36s	First	-2.506662	9.780426	9.77491053
22	T04F	36s	First	-2.664347	9.780439	9.77600066
23	T05F	36s	First	-2.436597	9.780420	9.77578315
24	T06F	36s	First	-2.067269	9.780394	9.77414940
25	T07F	36s	First	-2.742595	9.780445	9.77634528
26	T08F	36s	First	-3.593106	9.780530	9.77596304
27	T09F	36s	First	-3.335702	9.780502	9.77671546

4.1.6 Computed mean normal gravity and mean gravity of TAREF11 control points

The mean normal gravity ($\bar{\gamma}$) and mean gravity (\bar{g}) information used in this study were computed using equation 3.8 and equation 3.9 as explained in sect (3.6) and sect (3.7) respectively. The final results are in Table 4.6. Where, \bar{g} is the mean gravity along the plumb line between point and geoid and $\bar{\gamma}$ is the mean normal gravity along the plumb line between point and quasi geoid.

Table 4.6: Computed mean normal gravity and mean gravity values of TAREF11 controls

S/No	St/Name	Zone	Order	$\bar{\gamma}$ (m/s^2)	\bar{g} (m/s^2)
1	ARIT	36s	CORS	9.775066206	9.777119676
2	MOSH	37s	CORS	9.776532586	9.777956706
3	TANZ	37s	CORS	9.780592089	9.780782866
4	DARA	37s	CORS	9.780824016	9.780931493
5	ZNZB	37s	CORS	9.780819366	9.780798267
6	DODC	36s	CORS	9.775737120	9.777869285
7	T01Z	36s	Zero	9.779791989	9.780303136
8	T02Z	37s	Zero	9.779011442	9.780222564
9	T03Z	37s	Zero	9.781470968	9.781946495
10	T05Z	36S	Zero	9.774638876	9.777794035
11	T07Z	36s	Zero	9.772973545	9.777627379
12	T09Z	37s	Zero	9.780680603	9.780308322
13	T11Z	36s	Zero	9.775081728	9.777128604
14	T12Z	35s	Zero	9.776882827	9.777991181
15	T13Z	36s	Zero	9.774557339	9.776932337
16	T14Z	36S	Zero	9.775122344	9.777207220
17	T15Z	36S	Zero	9.774875082	9.776971447
18	T16Z	37s	Zero	9.778710616	9.779647504
19	T01F	36s	First	9.778664835	9.776100137
20	T02F	36s	First	9.772897549	9.776113829
21	T03F	36s	First	9.772152731	9.776155399
22	T04F	36s	First	9.773781736	9.776787698
23	T05F	36s	First	9.773464566	9.776578947
24	T06F	36s	First	9.771026637	9.775475503
25	T07F	36s	First	9.774295408	9.777053148
26	T08F	36s	First	9.773679678	9.776752985
27	T09F	36s	First	9.774822416	9.777245782
28	T10F	36s	First	9.774675081	9.777057225

4.1.7 Computed normal heights of TAREF11 control points Using Geopotential numbers

The normal heights in this study were computed using equation (2.6) as explained in sect (3.8) and the final results of the computed normal height using geopotential numbers are in Table 4.7.

Where, $H_{XGM2019e}^N$ is the normal height by fundamental approach, C_p is geopotential number and $\bar{\gamma}$ is the mean normal gravity along the plumb line between point and quasi geoid.

Table 4.7: Computed Normal height of TAREF11 controls using Geopotential number

S/No	St/Name	Zone	Order	C_p (m^2/s^2)	$\bar{\gamma}$ (m/s^2)	$H_{XGM2019e}^N$ (meter)
1	ARIT	36s	CORS	11956.78189	9.775066206	1223.192
2	MOSH	37s	CORS	8396.225720	9.776532586	858.214
3	TANZ	37s	CORS	955.44781	9.780592089	97.688
4	DARA	37s	CORS	487.73502	9.780824016	49.866
5	ZNZB	37s	CORS	232.58743	9.780819366	23.780
6	DODC	36s	CORS	10947.96787	9.77573712	1119.912
7	T01Z	36s	Zero	5295.8293	9.779791989	541.507
8	T02Z	37s	Zero	6798.33851	9.779011442	695.196
9	T03Z	37s	Zero	1091.67555	9.781470968	111.606
10	T05Z	36S	Zero	13968.26045	9.774638876	1428.030
11	T07Z	36s	Zero	17619.13327	9.772973545	1802.842
12	T09Z	37s	Zero	113.19232	9.780680603	11.573
13	T11Z	36s	Zero	11924.02733	9.775081728	1219.839
14	T12Z	35s	Zero	8053.18091	9.776882827	823.696
15	T13Z	36s	Zero	12244.00843	9.774557339	1252.641
16	T14Z	36S	Zero	11194.74961	9.775122344	1145.228
17	T15Z	36S	Zero	11589.69044	9.774875082	1185.661
18	T16Z	37s	Zero	4919.71744	9.778710616	503.104
19	T01F	36s	First	16115.97502	9.778664835	1648.075
20	T02F	36s	First	15803.44549	9.772897549	1617.068
21	T03F	36s	First	17468.55808	9.772152731	1787.585
22	T04F	36s	First	14056.70692	9.773781736	1438.205
23	T05F	36s	First	14693.4948	9.773464566	1503.406
24	T06F	36s	First	19780.44175	9.771026637	2024.397
25	T07F	36s	First	12991.34298	9.774295408	1329.133
26	T08F	36s	First	14467.46652	9.773679678	1480.247
27	T09F	36s	First	11994.62319	9.774822416	1227.093
28	T10F	36s	First	12322.11233	9.774675081	1260.616
29	T11F	36s	First	11957.58949	9.774843751	1223.302

4.1.8 Computed normal heights of TAREF11 control points using TZQ17 quasi-geoid model

The normal heights in this study were computed using equation (2.7) as explained in sect (3.9) and the final results of the computed normal height using TZQ17 are in Table 4.8 where, H_{TZQ17}^N is the normal height, h^{elp} is the ellipsoidal height of point on the topography obtained through GNSS positioning and ζ is the height anomaly extracted from TZQ17 quasi-geoid model.

Table 4.8: Computed Normal heights of TAREF11 controls Using TZQ17

S/No	St/Name	Zone	Order	h^{elp} (meter)	ζ (meter)	H_{TZQ17}^N (meter)
1	ARIT	36s	CORS	1204.850	-17.524	1222.374
2	MOSH	37s	CORS	840.602	-16.993	857.596
3	TANZ	37s	CORS	70.461	-27.052	97.512
4	DARA	37s	CORS	22.395	-27.418	49.813
5	ZNZB	37s	CORS	-3.975	-28.484	24.508
6	DODC	36s	CORS	1099.970	-20.217	1120.187
7	T01Z	36s	Zero	523.351	-18.459	541.810
8	T02Z	37s	Zero	672.877	-21.910	694.787
9	T03Z	37s	Zero	86.819	-25.046	111.866
10	T05Z	36S	Zero	1411.340	-16.296	1428.236
11	T07Z	36s	Zero	1791.212	-10.681	1801.894
12	T09Z	37s	Zero	-15.937	-27.267	11.330
13	T11Z	36s	Zero	1201.499	-17.524	1219.024
14	T12Z	35s	Zero	808.035	-16.761	823.796
15	T13Z	36s	Zero	1237.596	-14.576	1252.172
16	T14Z	36S	Zero	1127.871	-16.608	1144.479
17	T15Z	36S	Zero	1167.988	-17.602	1185.591
18	T16Z	37s	Zero	480.313	-22.769	503.082
19	T01F	36s	First	1635.792	-11.979	1647.772
20	T02F	36s	First	1599.796	-16.333	1616.129
21	T03F	36s	First	1776.226	-10.723	1786.950
22	T04F	36s	First	1424.586	-13.191	1437.778
23	T05F	36s	First	1486.401	-15.954	1502.355
24	T06F	36s	First	2007.758	-15.678	2023.436
25	T07F	36s	First	1312.080	-16.165	1328.245
26	T08F	36s	First	1467.568	-11.968	1479.536
27	T09F	36s	First	1212.647	-13.979	1226.626
28	T10F	36s	First	1243.647	-16.397	1260.045
29	T11F	36s	First	1204.496	-18.307	1222.803

4.1.9 Computed normal heights of TAREF11 control points using a strict formula

The normal heights in this study were computed using equation (2.14) as explained in sect (3.10) and the final results of the computed normal height using a strict formula are in table 4.9 where, H_{SGQS}^N is the normal height, h^{elp} is the ellipsoidal height of point on the topography obtained through GNSS positioning and ζ_{SGQS} is the height anomaly computed by a strict formula.

Table 4.9: Computed Normal height of TAREF11 control using strict formula

S/No	St/Name	Zone	N- ζ (meter)	ζ (meter)	h^{elp} (meter)	H_{SGQS}^N (meter)
1	ARIT	36s	-0.313	-18.358	1204.850	1223.208
2	MOSH	37s	-0.135	-17.887	840.603	858.490
3	TANZ	37s	0.011	-27.189	70.461	97.650
4	DARA	37s	0.006	-27.436	22.396	49.831
5	ZNZB	37s	0.003	-27.693	-3.976	23.717
6	DODC	36s	-0.229	-19.934	1099.971	1119.904
7	T01Z	36s	-0.044	-17.793	523.351	541.144
8	T02Z	37s	-0.051	-22.172	672.878	695.050
9	T03Z	37s	0.016	-24.695	86.819	111.514
10	T05Z	36s	-0.370	-17.663	1411.340	1429.003
11	T07Z	36s	-0.553	-11.947	1791.213	1803.160
12	T09Z	37s	0.001	-27.533	-15.937	11.596
13	T11Z	36s	-0.312	-18.356	1201.500	1219.856
14	T12Z	35s	-0.131	-15.565	808.035	823.601
15	T13Z	36s	-0.301	-15.064	1237.596	1252.660
16	T14Z	36s	-0.245	-17.309	1127.871	1145.180
17	T15Z	36s	-0.292	-17.741	1167.989	1185.730
18	T16Z	37s	-0.005	-22.571	480.314	502.884
19	T01F	36s	-0.538	-13.097	1635.793	1648.890
20	T02F	36s	-0.556	-17.346	1599.797	1617.143
21	T03F	36s	-0.599	-11.453	1776.227	1787.680
22	T04F	36s	-0.397	-13.689	1424.587	1438.275
23	T05F	36s	-0.441	-17.006	1486.401	1503.407
24	T06F	36s	-0.828	-16.643	2007.758	2024.401
25	T07F	36s	-0.317	-16.925	1312.080	1329.005
26	T08F	36s	-0.426	-12.876	1467.568	1480.444
27	T09F	36s	-0.283	-14.501	1212.647	1227.149

4.1.10 Computed orthometric height of TAREF11 control points using geopotential number

The Orthometric heights in this study were computed using equation (2.3) as explained in sect (3.11) and the final results of the computed Orthometric height using geopotential number are in Table 4.10 where, $H_{XGM2019e}^O$ is the Orthometric height, C_p is the geopotential number and \bar{g} is the mean gravity along the actual plumbline between the measured point and geoid.

Table 4.10: Computed Orthometric height using geopotential number

S/No	St/Name	Zone	Order	C_p (m^2/s^2)	\bar{g} (m/s^2)	$H_{XGM2019e}^O$ (meter)
1	ARIT	36s	CORS	11956.78189	9.777119676	1222.935
2	MOSH	37s	CORS	8396.22572	9.777956706	858.689
3	TANZ	37s	CORS	955.44781	9.780782866	97.686
4	DARA	37s	CORS	487.73502	9.780931493	49.865
5	ZNZB	37s	CORS	232.58743	9.780798267	23.780
6	DODC	36s	CORS	10947.96787	9.777869285	1119.668
7	T01Z	36s	Zero	5295.8293	9.780303136	541.479
8	T02Z	37s	Zero	6798.33851	9.780222564	695.111
9	T03Z	37s	Zero	1091.67555	9.781946495	111.601
10	T05Z	36S	Zero	13968.26045	9.777794035	1428.569
11	T07Z	36s	Zero	17619.13327	9.777627379	1801.984
12	T09Z	37s	Zero	113.19232	9.780308322	11.573
13	T11Z	36s	Zero	11924.02733	9.777128604	1219.583
14	T12Z	35s	Zero	8053.18091	9.777991181	823.602
15	T13Z	36s	Zero	12244.00843	9.776932337	1252.336
16	T14Z	36S	Zero	11194.74961	9.777207220	1144.984
17	T15Z	36S	Zero	11589.69044	9.776971447	1185.407
18	T16Z	37s	Zero	4919.71744	9.779647504	503.056
19	T01F	36s	First	16115.97502	9.776100137	1648.507
20	T02F	36s	First	15803.44549	9.776113829	1616.536
21	T03F	36s	First	17468.55808	9.776155399	1786.853
22	T04F	36s	First	14056.70692	9.776787698	1437.763
23	T05F	36s	First	14693.4948	9.776578947	1502.928
24	T06F	36s	First	19780.44175	9.775475503	2023.476
25	T07F	36s	First	12991.34298	9.777053148	1328.758
26	T08F	36s	First	14467.46652	9.776752985	1479.782
27	T09F	36s	First	11994.62319	9.777245782	1226.789
28	T10F	36s	First	12322.11233	9.777057225	1260.308
29	T11F	36s	First	11957.58949	9.777032855	1223.028

4.1.11 Computed orthometric height of TAREF11 control points using TZG17 geoid model

The Orthometric heights in this study were computed using equation (3.12) as explained in sect (3.12) and the final results of the computed Orthometric height using TZG17 geoid model are in Table 4.11 where, H_{TZG17}^O is the Orthometric height, h^{elp} is the ellipsoidal height of point on the topography obtained through GNSS positioning and N is the Geoidal undulation extracted from TZG17 geoid model.

Table 4.11: Computed Orthometric heights of TAREF11 controls from TZG17 geoid model

S/No	St/Name	Zone	Order	h^{elp} (meter)	N (meter)	H_{TZG17}^O (meter)
1	ARIT	36s	CORS	1204.850	-18.044	1222.894
2	MOSH	37s	CORS	840.602	-17.752	858.355
3	TANZ	37s	CORS	70.460	-27.200	97.661
4	DARA	37s	CORS	22.395	-27.441	49.837
5	ZNZB	37s	CORS	-3.975	-27.696	23.720
6	DODC	36s	CORS	1099.971	-19.704	1119.675
7	T01Z	36s	Zero	523.351	-17.748	541.099
8	T02Z	37s	Zero	672.877	-22.120	694.998
9	T03Z	37s	Zero	86.819	-24.710	111.529
10	T05Z	36S	Zero	1411.340	-17.292	1428.632
11	T07Z	36s	Zero	1791.212	-11.394	1802.606
12	T09Z	37s	Zero	-15.937	-27.533	11.596
13	T11Z	36s	Zero	1201.499	-18.044	1219.544
14	T12Z	35s	Zero	808.035	-15.433	823.469
15	T13Z	36s	Zero	1237.596	-14.762	1252.359
16	T14Z	36S	Zero	1127.871	-17.063	1144.934
17	T15Z	36S	Zero	1167.988	-17.449	1185.437
18	T16Z	37s	Zero	480.313	-22.566	502.879
19	T01F	36s	First	1635.792	-12.559	1648.352
20	T02F	36s	First	1599.796	-16.790	1616.586
21	T03F	36s	First	1776.226	-10.853	1787.080
22	T04F	36s	First	1424.586	-13.291	1437.877
23	T05F	36s	First	1486.401	-16.564	1502.965
24	T06F	36s	First	2007.758	-15.815	2023.573
25	T07F	36s	First	1312.080	-16.607	1328.688
26	T08F	36s	First	1467.568	-12.450	1480.018
27	T09F	36s	First	1212.647	-14.218	1226.865

4.1.12 Computed dynamic height of TAREF11 control points using geopotential number

The dynamic heights in this study were computed using equation (2.9) as explained in sect (3.13) and the final results of the computed dynamic height using geopotential number are in Table 4.12 where, H^D is the dynamic height, C_p is the geopotential number and γ_Q is normal gravity on telluroid computed using equation 3.5 in which key inputs were the constant normal gravity value γ_o , usually ϕ is 45° having a value of 980619.9877 mGal as computed using equation 3.6 and normal height (h_Q).

Table 4.12: Computed Dynamic heights of TAREF11 controls using geopotential number

S/No	St/Name	Zone	Order	C_p (m^2/s^2)	γ_Q (m/s^2)	H^D (meter)
1	ARIT	36s	CORS	11956.78189	9.802429328	1219.777
2	MOSH	37s	CORS	8396.22572	9.803554302	856.447
3	TANZ	37s	CORS	955.44781	9.805899009	97.436
4	DARA	37s	CORS	487.73502	9.806046179	49.738
5	ZNZB	37s	CORS	232.58743	9.806124257	23.718
6	DODC	36s	CORS	10947.96787	9.802744451	1116.826
7	T01Z	36s	Zero	5295.8293	9.804528338	540.141
8	T02Z	37s	Zero	6798.33851	9.804056463	693.420
9	T03Z	37s	Zero	1091.67555	9.805854724	111.328
10	T05Z	36S	Zero	13968.26045	9.801796385	1425.071
11	T07Z	36s	Zero	17619.13327	9.800642487	1797.752
12	T09Z	37s	Zero	113.19232	9.806164917	11.542
13	T11Z	36s	Zero	11924.02733	9.802439659	1216.434
14	T12Z	35s	Zero	8053.18091	9.803655464	821.446
15	T13Z	36s	Zero	12244.00843	9.802337439	1249.090
16	T14Z	36S	Zero	11194.74961	9.802669540	1142.010
17	T15Z	36S	Zero	11589.69044	9.802542758	1182.314
18	T16Z	37s	Zero	4919.71744	9.804647802	501.774
19	T01F	36s	First	16115.97502	9.801117649	1644.299
20	T02F	36s	First	15803.44549	9.801215205	1612.396
21	T03F	36s	First	17468.55808	9.800688560	1782.380
22	T04F	36s	First	14056.70692	9.801765114	1434.099
23	T05F	36s	First	14693.4948	9.801565998	1499.096
24	T06F	36s	First	19780.44175	9.799959534	2018.420
25	T07F	36s	First	12991.34298	9.802102859	1325.362

4.2 Statistical analysis of Normal heights differences of TAREF11 controls

Golden surfer software version 18 grid math module was used to compare and assess statistically the fit between the normal heights pair. Comparison was made between the computed normal heights using geopotential number, TZQ 17 and a strict formula. Normal heights computed by a strict formula was used to validate the quality of geopotential number and TZQ17 respectively. The statistic values obtained from the computed normal height using geopotential number, TZQ 17 and a strict formula are shown in Table 4.13 below.

Table 4.13: Statistic of computed normal heights of TAREF11 controls

STATISTIC	$H_{XGM2019e}^N$	H_{TZQ17}^N	H_{SGQS}^N
Number of values	577	577	577
Sum	574183.931	573937.842	574138.892
Minimum	3.011	3.273	3.114
Maximum	2745.857	2745.138	2746.059
Mean	995.119	994.693	995.041
Standard deviation	539.375	539.161	539.406
Root Mean Square:	1131.896	1131.418	1131.842

The statistics of the residuals obtained after subtracting heights values from one height system to another are shown in Table (4-14). Where, $\Delta H1$ is the difference of normal height between geopotential numbers ($H_{XGM2019e}^N$) and TZQ17 (H_{TZQ17}^N), $\Delta H2$ is the difference between geopotential numbers ($H_{XGM2019e}^N$) and a strict formula (H_{SGQS}^N) and $\Delta H3$ is the difference of normal height between TZQ17 (H_{TZQ17}^N) and a strict formula (H_{SGQS}^N) respectively.

Table 4.14: Statistical analysis of TAREF11 controls normal heights differences

STATISTIC	$\Delta H1$ (meter)	$\Delta H2$ (meter)	$\Delta H3$ (meter)
Number of values	577	577	577
Sum	246.088	45.039	201.049
Minimum	-1.084	-0.814	-0.851
Maximum	1.406	1.115	1.632
Mean	0.426	0.078	0.348
Standard deviation	0.456	0.193	0.448
Root Mean Square:	0.458	0.194	0.450

Furthermore, to remove outliers from our study a test was conducted at 95% confidence interval to see how significantly consistency the results are at that confidence interval. Table 4.15 shows the statistical analysis of normal heights difference at 95% confidence level.

Table 4.15: Statistic analysis of normal heights differences at 95% confidence interval

STATISTIC AT 95% CI	$\Delta H1$ (meter)	$\Delta H2$ (meter)	$\Delta H3$ (meter)
Number of values	40	46	38
Number of missing values	537	531	539
Sum	17.048	3.577	13.374
Minimum	0.395	0.062	0.314
Maximum	0.464	0.093	0.384
Mean	0.426	0.077	0.352
Standard deviation	0.019	0.009	0.012
Root Mean Square:	0.426	0.078	0.352

4.3 Statistical analysis of Orthometric heights differences of TAREF11 controls

Comparison was made between the computed orthometric heights using geopotential number, TZG17 and GPS levelling. The comparison was done so as check if the results between these heights are significantly consistent. TZG17 orthometric heights was used to validate orthometric heights computed using geopotential number. Golden surfer software version 18 grid math module was used to compare and assess statistically the fit between the orthometric heights pair. The statistic values obtained from the computed Orthometric height using GPS levelling, XGM2019e_5540 and TZG17 are shown in Table 4.16 below.

Table 4.16: Statistic of computed Orthometric heights of TAREF11 controls

STATISTIC	H_{GPS}^0	$H_{XGM2019e}^0$	H_{TZG17}^0
Number of values	577	577	577
Sum	574531.525	574035.733	573997.231
Minimum	3.933	3.011	3.114
Maximum	2744.611	2743.948	2744.057
Mean	995.722	994.862	994.795
Standard deviation	539.141	539.158	539.179
Root Mean Square:	1132.314	1131.566	1131.518

The statistics of the residuals obtained after subtracting heights values from one height system to another are shown in Table (4.17). Where, $\Delta H1$ is the difference of Orthometric height between those of GPS levelling (H_{GPS}^O) and geopotential numbers ($H_{XGM2019e}^O$), $\Delta H2$ is between those of GPS (H_{GPS}^O) and TZG17 (H_{TZG17}^O) and $\Delta H3$ is between those of geopotential numbers ($H_{XGM2019e}^O$) and TZG17 geoid model (H_{TZG17}^O) respectively.

Table 4.17: Statistical analysis of TAREF11 controls Orthometric heights differences

STATISTIC	$\Delta H1$ (meter)	$\Delta H2$ (meter)	$\Delta H3$ (meter)
Number of values	577	577	577
Sum	495.792	534.294	38.501
Minimum	-1.345	-1.309	-0.441
Maximum	1.849	1.931	0.494
Mean	0.859	0.925	0.066
Standard deviation	0.234	0.285	0.155
Root Mean Square:	0.890	0.969	0.168

To remove outliers from our study a test was conducted at 95% confidence interval to see how significantly consistency the results are at that confidence interval. Table 4.16 shows the statistical analysis of Orthometric heights difference at 95% confidence level.

Table 4.18: Statistic analysis of orthometric heights differences at 95% confidence interval

STATISTIC AT 95% CI	$\Delta H1$ (meter)	$\Delta H2$ (meter)	$\Delta H3$ (meter)
Number of values	79	58	49
Number of missing values	498	519	528
Sum	67.815	53.608	3.336
Minimum	0.840	0.903	0.055
Maximum	0.878	0.949	0.079
Mean	0.858	0.924	0.068
Standard deviation	0.010	0.012	0.006
Root Mean Square:	0.858	0.924	0.068

4.4 Discussion of the results

Table 4-14 in sect 4.2 shows the statistical analysis for computed normal heights differences using geopotential number, TZQ 17 quasi-geoid model and a strict formula. Based on the statistics, normal height computed using XGM2019e_5540 and a strict formula agree with one another,

followed by those computed by TZQ17 quasi-geoid model and a strict formula. Normal heights difference of XGM2019e_5540 and TZQ17 are not statistically consistent to those of TZQ17 and a strict formula and XGM2019e_5540 and a strict formula.

A test conducted at 95% confidence interval shows that there is a significance difference of 9.1mm between the normal height computed using geopotential number and a strict formula with a RMS of 7cm and 1.2 cm by those computed by TZQ17 and a strict formula with RMS of 35cm. Normal heights differences between XGM2019e_5540 and TZQ17 are still not statistically fit compared to those of a strict formula. These differences are contributed due to difference in datum and model accuracies between these three heights methods.

From the results obtained, Assessment done with respect to normal heights computed by a strict formula, normal height computed using geopotential number yield better results followed by those of TZQ17 quasi-geoid model. XGM2019e_5540 and a strict formula better result was due to likeliness of formula used in computation of these height final results.

Table 4-16 in sect 4.3 shows the statistical analysis for computed orthometric heights differences using GPS levelling, XGM2019e_5540 and TZG17. Based on the statistics orthometric height computed using XGM2019e_5540 and TZG17 geoid model agree with one another, followed by those computed by GPS levelling and XGM2019e_5540. Orthometric heights difference of GPS levelling and TZG17 are not statistically consistent with those of XGM2019e_5540 and TZG17 geoid model.

A test conducted at 95% confidence interval shows that there is a significance difference 6.85mm between the orthometric height computed by using XGM2019e_5540 and TZG17 with a RMS of 6.8 cm and 1cm by those computed by GPS levelling and XGM2019e_5540 with RMS of 85.85cm. orthometric heights difference of GPS levelling and TZG17 are still not statistically fit compared to those of XGM2019e_5540 and TZG17. These differences are contributed due to difference in datum and model accuracies between these three heights methods.

From the results obtained, Assessment done with respect to orthometric heights computed by TZG17 geoid model showed that orthometric heights computed with GPS levelling didn't statistical fit best with other. Furthermore, Orthometric height computed by using XGM2019e_5540 model is statistical fit at 6mm to those of TZG17.

CHAPTER FIVE

CONCLUSION AND RECOMMENDATION

5.1 Conclusion

Dynamic height, orthometric and normal heights were successfully computed and analyzed. Validation of orthometric and normal heights was done using TZG17 geoid model and a strict formula respectively. Assessment of the orthometric and normal height was done based on statistical analyses in which a test was conducted at 95% and the results showed there is a significance difference of 9.1mm between the normal height computed using geopotential number and a strict formula and 1.2 cm by those computed by TZQ17 and a strict formula. Also, there is a significance difference of 6.85mm between the orthometric height computed by using XGM2019e_5540 and TZG17 and 1cm by those computed by TAREF11 GPS levelling and XGM2019e_5540.

Determination of TAREF11 controls geopotential (dynamic) heights will help not only geodesists but also field surveyors and engineers during construction of structure mostly related to hydrodynamics and energetics of transporting mass such as construction of canals, dams and pipeline which requires the potential to be evaluated on or above the Earth's surface. Furthermore, Normal and Orthometric heights can be used for realization of physical height systems.

5.2 Recommendations

Based from the results and discussion in chapter four above and conclusion made in chapter five the following are recommended.

- a) Since long, it has been known that a strict formula is not accurate enough for precise height conversion in mountainous regions. Therefore, validation of these normal heights, especially for mountainous area like as Mbinga should be done by conducting static GNSS (GPS) observations on some of TAREF11 control points for a minimum of 6-hours to obtain reliable assessment results.
- b) Since geopotential heights depends on local vertical datum then, there should be improvement on Local Geopotential Vertical Datum ($W_0^{LVD, TZG17}$) using the latest Gravimetric Geoid Models for Tanzania (TZG19 and others). Also new GPS observation should be done at Tanga Tide Gauge Benchmark (TGBM).

REFERENCES

- Abdalla, A. (2009). Determination of a Gravimetric Geoid Model of Sudan Using the KTH Method. A M.Sc. Thesis in Geodesy No. 3109. Stockholm, Sweden: Royal Institute of Technology (KTH).
- Andersen, O.B., & Knudsen P. (2000). The role of satellite altimetry in gravity field modelling in coastal areas. *physics and Chemistry of the Earth*, 25(1), 17-24.
- Baarda, W. (1968). A Testing Procedure for Use in Geodetic Networks. *Geodesy, New Series*, Vol. 2, No. 5
- Balmino, G., Vales, N.B., & Briais, A. (2011). Spherical harmonic modeling to ultra-degree of Bouguer and isostatic anomalies. *Journal of Geodesy*, pp (1-3).
- Bedada, T. B. (2010). An Absolute Geopotential Height System for Ethiopia. Edinburgh Scotland: Doctorate thesis, University of Edinburgh. Scotland.
- Delgado, R. E. & Rodrigues, T. L. (2022). Use of GNSS and a refined GGM (XGM2019e) for determining normal heights in the Imbituba Brazilian Vertical Datum and in the International Height Reference System. *Bulletin of Geodetic Sciences*. 28(2): e2022009, 2022.
- Deus, D. (2007). Determination of transformation parameters between the Tanzania national levelling datum and the Geoid. MSc. dissertation of SGST. Dar es Salaam, Tanzania: Ardhi University.
- Featherstone, W.E. & Kuhn M. (2006). Height systems and vertical datums: a review in the Australian context. *Journal of Spatial Sciences*. 51 (1): pp. 21-41.
- Featherstone, W. E. & Filmer, M. S. (2012). Three viable options for a new Australian vertical datum. *Journal of Spatial Science*, 19-36.
- Filmer, M. S., Featherstone, W. E., Brown, N. J., & McCubbine, J. C. (2018). Description and release of Australian gravity field model testing data. *Australian Journal of Earth Sciences*, 1-7.

- Flury, J. & Rummel, R (2009). On the geoid-quasigeoid separation in mountain areas. *Journal of Geodesy* 83, 829.
- Flury, J. & Rummel, R (2011). On the computation of the geoid–quasigeoid separation Response to “A strict formula for geoid-to-quasigeoid separation” by Lars Sjöberg. *Journal of Geodesy* 85:185–186.
- Foroughi, I., Vanicek, P., Sheng, M., Kingdon, R. W., & Santos, M. C. (2017). In defense of the classical height system. *Journal of Geophysics*. 211(2): 1154-61
- Heiskanen, W.A. and Moritz, H. (1967) *Physical Geodesy*, WH Freeman & Co, San Francisco, USA, 364 pp.
- Hofmann-Wellenhof, B., & Moritz, H. (2005). *Physical Geodesy*. Technische Universität Graz, Graz, Austria: SpringerWienNewYork.
- Lwehumbiza, L. (2017). Evaluation of recent GRACE and or GOCE GGMs over Tanzania using terrestrial gravity data. A Dissertation Submitted in Partial Fulfillment of the Requirements for the Award of Bachelor of Science Degree in Geomatics. Dar-es-salaam: Ardhi University.
- Masunga, E. (2016). Optimal Geopotential Vertical Datum for Tanzania from TZG13 Gravimetric Geoid Model together with GPS and Oceanic Levelling. MSc. dissertation of SGST. Dar es Salaam, Tanzania: Ardhi University.
- Mayunga, M. S. (2016). Towards a New Geoid Model of Tanzania using Precise Gravity Data. *Journal of Environmental Science and Engineering*, 267-276.
- Melitha, G. (2020). corrector surface for optimal orthometric height compatible to Tanzania height system using Tzg13, Tzg17 and Tzg19 geoid Models. A B.Sc. Dissertation of the department of Geospatial Sciences and Technology (B.Sc. GM). Dar-es-salaam: Ardhi University. Tanzania
- Molodensky, M., Yeremeyev, V. and Yurkina, M. (1962) *Methods for Study of the External Gravitational field and Figure of the Earth*, Israeli Program for Scientific Translations, Jerusalem, 236pp.

- Mtamakaya, J. D. (2009). Establishment and Maintenance of a New Geospatial Frame for Tanzania-TZRF10. M.Sc. dissertation Canada: Department of Geodesy and Geomatics Engineering. New Brunswick University. Canada.
- Muhammad, S., Zulfiqar, A., & Gulraiz, A. (2009). A study on the evaluation of the geoid-Quasigeoid separation term over Pakistan with a solution of first and second order height terms. *Earth planets space*, 61,815-823.
- Peter, R. V. (2018). Tanzania Gravimetric Geoid Model (TZG17) Through Quasi-Geoid by the KTH Method. MSc. dissertation of SGST. Dar es Salaam, Tanzania: Ardhi University.
- Sadiq, M., Ahmad, Z., & Akhter, G. (2009). A study on evaluation of the geoid-quasi geoid separation term over Pakistan with a solution of first and second order height terms. *Journal of Earth, Planets and Space*, 61(815-823).
- Sanchez, L. (2013). Classical height systems, Vertical datum standardization (unification), Towards a modern vertical reference system. 11th International School of the Geoid Service: heights and height datum, Loja, Ecuador, October 7–13, 2013.
- Sjöberg, L. E. (2007). The topographic bias by analytical continuation in physical geodesy. *Journal of Geodesy*, 81:345-350.
- Sjöberg, L. E. (2010). A “strict” formula for geoid-to-quasigeoid separation. *Journal of Geodesy*, 84:699-702.
- Sjöberg, L. E. (2013). The geoid or quasigeoid which reference surface should be preferred for a national height system? *Journal of Geodetic science*, 2013:103-109.
- Sjöberg, L. E. (2015). Rigorous geoid from quasigeoid correction using gravity disturbances *Journal of Geodetic science*, 2015;5:115–118.
- Ssengendo, R., Sjöberg, L. E., & Gidudu, A. (2015). Computation of the Gravimetric Quasigeoid Model over Uganda Using the KTH Method. Sofia, Bulgaria, 17-21 May 2015: FIG Working Week 2015.

- Sjöberg, L. E. and Bagherbandi M. (2017). Gravity inversion and integration, Theory and Applications in Geodesy and Geophysics. Basel, Switzerland: Springer International Publishing AG. https://doi.org/10.1007/978-3-319-50298-4_6.
- Sjöberg, L. E. (2018). On the geoid and orthometric height vs. quasigeoid and normal height. *Journal of Geodesy*, 2018;8:115–120.
- Torge, W. (2001). *Geodesy* (3rd ed., pp. 416). Berlin, New York, Germany: Walter de Gruyter publisher. <https://doi.org/10.1515/9783110879957>.
- Ulotu, P. E. (2009). Geoid Model of Tanzania from Sparse and Varying Gravity Data Density by the KTH Method. 10044 Stockholm, Sweden.: PhD thesis, Royal Institute of Technology (KTH).
- Ulotu, P. E. (2015). Optimal Vertical Datum for Tanzania. *JLAEA*, Vol. 3, Issue 2, pp. 225-235.
- Wang, Y. M., Veronneau, M., Huang, J., Ahlgren, K., Krcmaric, J., Xiaopeng, L., & Avalos-Naranjo, D. (2023). Accurate computation of geoid-quasigeoid separation in mountainous region—A case study in Colorado with full extension to the experimental geoid region. *Journal of Geodetic science*, 2023; 13: 20220128.
- Zingerle, P., Pail, R., Gruber, T., & Oikonomidou, X. (2020). The Combined global gravity field model XGM2019e . *Journal of Geodesy*, 66 (94).

APPENDICES

APPENDIX 1: CORS and Zero order data extracted from XGMe2019 model

Software	2.1.4 (GUI used)
Computer name	DESKTOP-1IHM3TF
Generating date	18-Apr-2023
Generating time	18:26:47
MATLAB version	9.0.0.341360 (R2016a)
Computed	Functionals of the geopotential
Imported data file	D:\TAREF11\CORSZERO.csv
Geopotential model file	D:\TAREF11\XGM2019e.gfc
GM of the geopotential model (m^3*s^{-2})	3.98600441500000e+14
R of the geopotential model (m)	6.37813630000000e+06
Minimum used degree	0
Maximum used degree	5540
Reference ellipsoid	GRS80
Type of the input coordinates	Ellipsoidal
Latitude limit North (deg)	-1.32554693900000e+00
Latitude limit South (deg)	-1.12736729100000e+01
Longitude limit West (deg)	2.96683632500000e+01
Longitude limit East (deg)	4.01849436900000e+01
Number of points	18
Computation time (dd:hh:mm:ss)	00:00:01:31
Computation of fully normalized ALFs	Standard forward column method

Exported data file contains the following columns:

Ellipsoidal Latitude (deg) Longitude (deg) Height above the reference ellipsoid (m) Gravity (mGal) Gravity_potential (m^2*s^{-2})

-5.04E+00	3.28E+01	1.20E+03	9.78E+05	6.26E+07
-3.35E+00	3.73E+01	8.41E+02	9.78E+05	6.26E+07
-6.77E+00	3.92E+01	7.05E+01	9.78E+05	6.26E+07
-6.82E+00	3.93E+01	2.24E+01	9.78E+05	6.26E+07
-6.22E+00	3.92E+01	-3.98E+00	9.78E+05	6.26E+07
-6.17E+00	3.57E+01	1.10E+03	9.78E+05	6.26E+07
-1.13E+01	3.48E+01	5.23E+02	9.78E+05	6.26E+07
-1.11E+01	3.73E+01	6.73E+02	9.78E+05	6.26E+07
-1.03E+01	4.02E+01	8.68E+01	9.78E+05	6.26E+07
-7.68E+00	3.58E+01	1.41E+03	9.78E+05	6.26E+07
-7.95E+00	3.16E+01	1.79E+03	9.78E+05	6.26E+07
-5.09E+00	3.91E+01	-1.59E+01	9.78E+05	6.26E+07
-5.04E+00	3.28E+01	1.20E+03	9.78E+05	6.26E+07
-4.89E+00	2.97E+01	8.08E+02	9.78E+05	6.26E+07
-1.33E+00	3.18E+01	1.24E+03	9.78E+05	6.26E+07
-2.45E+00	3.29E+01	1.13E+03	9.78E+05	6.26E+07
-1.54E+00	3.38E+01	1.17E+03	9.78E+05	6.26E+07
-6.75E+00	3.78E+01	4.80E+02	9.78E+05	6.26E+07

APPENDIX 2: FIRST order data extracted from XGMe2019 model

Software	2.1.4 (GUI used)
Computer name	DESKTOP-1IHM3TF
Generating date	18-Apr-2023
Generating time	18:38:57
MATLAB version	9.0.0.341360 (R2016a)
Computed	Functionals of the geopotential
Imported data file	D:\TAREF11\FIRST ORDER.csv
Geopotential model file	D:\TAREF11\XGM2019e.gfc
GM of the geopotential model (m^3*s^{-2})	3.98600441500000e+14
R of the geopotential model (m)	6.37813630000000e+06
Minimum used degree	0
Maximum used degree	5540
Reference ellipsoid	GRS80
Type of the input coordinates	Ellipsoidal
Latitude limit North (deg)	-1.53189761900000e+00
Latitude limit South (deg)	-1.15810825000000e+01
Longitude limit West (deg)	3.02745071800000e+01
Longitude limit East (deg)	3.95443276900000e+01
Number of points	72
Computation time (dd:hh:mm:ss)	00:00:01:53
Computation of fully normalized ALFs	Standard forward column method

Exported data file contains the following columns:

Ellipsoidal Latitude (deg) Longitude (deg) Height above the reference ellipsoid (m) Gravity (mGal) Gravity_potential (m^2*s^{-2})

-1.53E+00	3.12E+01	1.64E+03	9.78E+05	6.26E+07
-1.83E+00	3.47E+01	1.60E+03	9.78E+05	6.26E+07

-2.51E+00	3.07E+01	1.78E+03	9.78E+05	6.26E+07
-2.66E+00	3.14E+01	1.42E+03	9.78E+05	6.26E+07
-2.44E+00	3.48E+01	1.49E+03	9.78E+05	6.26E+07
-2.07E+00	3.55E+01	2.01E+03	9.77E+05	6.26E+07
-2.74E+00	3.67E+01	1.31E+03	9.78E+05	6.26E+07
-3.59E+00	3.07E+01	1.47E+03	9.78E+05	6.26E+07
-3.34E+00	3.15E+01	1.21E+03	9.78E+05	6.26E+07
-3.41E+00	3.24E+01	1.24E+03	9.78E+05	6.26E+07
-3.37E+00	3.34E+01	1.20E+03	9.78E+05	6.26E+07
-3.52E+00	3.43E+01	1.18E+03	9.78E+05	6.26E+07
-3.34E+00	3.57E+01	1.51E+03	9.78E+05	6.26E+07
-3.44E+00	3.67E+01	1.23E+03	9.78E+05	6.26E+07
-4.48E+00	3.03E+01	1.35E+03	9.78E+05	6.26E+07
-5.05E+00	3.13E+01	1.07E+03	9.78E+05	6.26E+07
-4.28E+00	3.29E+01	1.19E+03	9.78E+05	6.26E+07
-4.53E+00	3.34E+01	1.25E+03	9.78E+05	6.26E+07
-4.81E+00	3.47E+01	1.48E+03	9.78E+05	6.26E+07
-4.90E+00	3.58E+01	1.38E+03	9.78E+05	6.26E+07
-4.21E+00	3.69E+01	1.42E+03	9.78E+05	6.26E+07
-4.51E+00	3.79E+01	6.24E+02	9.78E+05	6.26E+07
-4.80E+00	3.83E+01	1.36E+03	9.78E+05	6.26E+07
-5.61E+00	3.05E+01	1.29E+03	9.78E+05	6.26E+07
-5.33E+00	3.17E+01	1.08E+03	9.78E+05	6.26E+07
-5.61E+00	3.27E+01	1.16E+03	9.78E+05	6.26E+07
-5.32E+00	3.32E+01	1.19E+03	9.78E+05	6.26E+07
-5.70E+00	3.45E+01	1.29E+03	9.78E+05	6.26E+07
-5.97E+00	3.60E+01	1.05E+03	9.78E+05	6.26E+07
-5.30E+00	3.66E+01	1.52E+03	9.78E+05	6.26E+07

APPENDIX 3: SECOND order data extracted from XGMe2019 model

Software	2.1.4 (GUI used)
Computer name	DESKTOP-1IHM3TF
Generating date	18-Apr-2023
Generating time	19:26:03
MATLAB version	9.0.0.341360 (R2016a)
Computed	Functionals of the geopotential
Imported data file	D:\TAREF11\SECOND ORDER.csv
Geopotential model file	D:\TAREF11\XGM2019e.gfc
GM of the geopotential model (m^3*s^{-2})	3.98600441500000e+14
R of the geopotential model (m)	6.37813630000000e+06
Minimum used degree	0
Maximum used degree	5540
Reference ellipsoid	GRS80
Type of the input coordinates	Ellipsoidal
Latitude limit North (deg)	-1.03730125100000e+00
Latitude limit South (deg)	-1.11426136100000e+01
Longitude limit West (deg)	3.05149506200000e+01
Longitude limit East (deg)	4.03463781300000e+01
Number of points	487
Computation time (dd:hh:mm:ss)	00:00:05:21
Computation of fully normalized ALFs	Standard forward column method

Exported data file contains the following columns:

Ellipsoidal Latitude (deg) Longitude (deg) Height above the reference ellipsoid (m) Gravity (mGal) Gravity_potential (m^2*s^{-2})

-6.58E+00	3.90E+01	4.01E+01	9.78E+05	6.26E+07
-6.61E+00	3.91E+01	1.27E+01	9.78E+05	6.26E+07

-6.67E+00	3.92E+01	9.66E+01	9.78E+05	6.26E+07
-6.67E+00	3.92E+01	1.00E+02	9.78E+05	6.26E+07
-6.77E+00	3.92E+01	7.37E+01	9.78E+05	6.26E+07
-6.78E+00	3.92E+01	1.06E+02	9.78E+05	6.26E+07
-6.80E+00	3.92E+01	7.98E+01	9.78E+05	6.26E+07
-6.78E+00	3.93E+01	-1.59E+01	9.78E+05	6.26E+07
-6.70E+00	3.91E+01	9.00E+01	9.78E+05	6.26E+07
-6.89E+00	3.91E+01	1.16E+02	9.78E+05	6.26E+07
-6.88E+00	3.92E+01	6.01E+01	9.78E+05	6.26E+07
-6.86E+00	3.93E+01	2.60E+01	9.78E+05	6.26E+07
-6.94E+00	3.93E+01	1.56E+01	9.78E+05	6.26E+07
-6.85E+00	3.94E+01	-1.23E+01	9.78E+05	6.26E+07
-6.87E+00	3.94E+01	2.47E+01	9.78E+05	6.26E+07
-6.89E+00	3.95E+01	-1.48E+01	9.78E+05	6.26E+07
-6.95E+00	3.92E+01	3.44E+01	9.78E+05	6.26E+07
-6.96E+00	3.93E+01	3.47E+01	9.78E+05	6.26E+07
-6.96E+00	3.94E+01	1.01E+02	9.78E+05	6.26E+07
-7.01E+00	3.95E+01	2.53E+01	9.78E+05	6.26E+07
-6.99E+00	3.95E+01	-6.19E+00	9.78E+05	6.26E+07
-7.53E+00	3.64E+01	5.48E+02	9.78E+05	6.26E+07
-7.49E+00	3.76E+01	1.54E+02	9.78E+05	6.26E+07
-7.28E+00	3.88E+01	4.29E+02	9.78E+05	6.26E+07
-7.66E+00	3.92E+01	1.17E+02	9.78E+05	6.26E+07
-6.87E+00	3.94E+01	-2.47E+01	9.78E+05	6.26E+07
-1.09E+01	3.50E+01	1.33E+03	9.78E+05	6.26E+07
-1.07E+01	3.52E+01	9.29E+02	9.78E+05	6.26E+07
-1.08E+01	3.47E+01	4.66E+02	9.78E+05	6.26E+07
-1.05E+01	3.49E+01	9.31E+02	9.78E+05	6.26E+07

APPENDIX 4: Bouguer gravity anomalies extracted from WGM12 model

BGI - BUREAU GRAVIMETRIQUE INTERNATIONAL / INTERNATIONAL
GRAVIMETRIC BUREAU

WGM2012 - Complete spherical Bouguer gravity anomaly

Model : WGM2012_Bouguer_ponc_2min

Grid Limits : LON [28/42] - LAT [-12/0]

LON(Deg) LAT(Deg) GRAVITY(mGal)

28	0	39.56	29.8	-4.633333333	-23.43
28.03333333	0	34.73	29.83333333	-4.633333333	-15.88
28.06666667	0	37.66	29.86666667	-4.633333333	-24.88
28.1	0	40.84	29.9	-4.633333333	-29.95
28.13333333	0	46.08	29.93333333	-4.633333333	-17.76
28.16666667	0	45.23	29.96666667	-4.633333333	-15.01
28.2	0	49.59	30	-4.633333333	-21.24
28.23333333	0	54.96	30.03333333	-4.633333333	-21.11
28.26666667	0	57.43	30.06666667	-4.633333333	-29.92
28.3	0	57.75	30.1	-4.633333333	-30.33
28.33333333	0	61.11	30.13333333	-4.633333333	-24.64
28.36666667	0	61	30.16666667	-4.633333333	-27.11
28.4	0	62.93	30.2	-4.633333333	-28.52
28.43333333	0	60.52	30.23333333	-4.633333333	-29.03
28.46666667	0	59.4	30.26666667	-4.633333333	-29.25
28.5	0	61.73	30.3	-4.633333333	-34.77
28.53333333	0	57.35	30.33333333	-4.633333333	-28.45
28.56666667	0	55.36	30.36666667	-4.633333333	-25.17
28.6	0	53.63	30.4	-4.633333333	-23.69
28.63333333	0	46.92	30.43333333	-4.633333333	-22
28.66666667	0	43.1	30.46666667	-4.633333333	-21.45

28.7	0	42.92	30.5	-4.633333333	-24.85
28.73333333	0	36.75	30.53333333	-4.633333333	-18.18
28.76666667	0	32.9	30.56666667	-4.633333333	-15.2
28.8	0	28.63	30.6	-4.633333333	-19.58
28.83333333	0	27.1	30.63333333	-4.633333333	-20.83
28.86666667	0	33.24	30.66666667	-4.633333333	-20.11
28.9	0	29.73	30.7	-4.633333333	-19.51
28.93333333	0	20.69	30.73333333	-4.633333333	-20.95
28.96666667	0	19.9	30.76666667	-4.633333333	-18.39
29	0	18.36	30.8	-4.633333333	-21.38
29.03333333	0	19.58	30.83333333	-4.633333333	-22.14
29.06666667	0	14.01	30.86666667	-4.633333333	-23.64
29.1	0	9.18	30.9	-4.633333333	-24.34
29.13333333	0	9.14	30.93333333	-4.633333333	-24.6
29.16666667	0	-0.41	30.96666667	-4.633333333	-24.53
29.2	0	-2.36	31	-4.633333333	-24.44
29.23333333	0	6.06	31.03333333	-4.633333333	-25.4
29.26666667	0	7.89	31.06666667	-4.633333333	-22.39
29.3	0	-3.69	31.1	-4.633333333	-21.21
29.33333333	0	-7.35	31.13333333	-4.633333333	-21.34
29.36666667	0	5.09	31.16666667	-4.633333333	-20.45
29.4	0	-1.95	31.2	-4.633333333	-17.49
29.43333333	0	-4.22	31.23333333	-4.633333333	-14.1
29.46666667	0	-9.84	31.26666667	-4.633333333	-11.56
29.5	0	-1.59	31.3	-4.633333333	-10.17
29.53333333	0	-6.51	31.33333333	-4.633333333	-9.12
29.56666667	0	-15.82	31.36666667	-4.633333333	-7.63
29.6	0	-9.91	31.4	-4.633333333	-4.62

APPENDIX 5: Computed Geopotential numbers of TAREF11 control points

S/No	St/Name	Zone	Order	Gravity Potential (Wp) (m^2/s^2)	($W_0^{LVD, TZG17}$) (m^2/s^2)	Geopotential Number (Cp) (m^2/s^2)
1	ARIT	36s	CORS	62624895.64	62636852.42	11956.78189
2	MOSH	37s	CORS	62628456.19	62636852.42	8396.22572
3	TANZ	37s	CORS	62635896.97	62636852.42	955.44781
4	DARA	37s	CORS	62636364.68	62636852.42	487.73502
5	ZNZB	37s	CORS	62636619.83	62636852.42	232.58743
6	DODC	36s	CORS	62625904.45	62636852.42	10947.96787
7	T01Z	36s	Zero	62631556.59	62636852.42	5295.8293
8	T02Z	37s	Zero	62630054.08	62636852.42	6798.33851
9	T03Z	37s	Zero	62635760.74	62636852.42	1091.67555
10	T05Z	36S	Zero	62622884.16	62636852.42	13968.26045
11	T07Z	36s	Zero	62619233.29	62636852.42	17619.13327
12	T09Z	37s	Zero	62636739.23	62636852.42	113.19232
13	T11Z	36s	Zero	62624928.39	62636852.42	11924.02733
14	T12Z	35s	Zero	62628799.24	62636852.42	8053.18091
15	T13Z	36s	Zero	62624608.41	62636852.42	12244.00843
16	T14Z	36S	Zero	62625657.67	62636852.42	11194.74961
17	T15Z	36S	Zero	62625262.73	62636852.42	11589.69044
18	T16Z	37s	Zero	62631932.7	62636852.42	4919.71744
19	T01F	36s	First	62620736.44	62636852.42	16115.97502
20	T02F	36s	First	62621048.97	62636852.42	15803.44549
21	T03F	36s	First	62619383.86	62636852.42	17468.55808
22	T04F	36s	First	62622795.71	62636852.42	14056.70692
23	T05F	36s	First	62622158.93	62636852.42	14693.4948
24	T06F	36s	First	62617071.98	62636852.42	19780.44175
25	T07F	36s	First	62623861.08	62636852.42	12991.34298
26	T08F	36s	First	62622384.95	62636852.42	14467.46652
27	T09F	36s	First	62624857.8	62636852.42	11994.62319
28	T10F	36s	First	62624530.31	62636852.42	12322.11233
29	T11F	36s	First	62624894.83	62636852.42	11957.58949
30	T12F	36s	First	62625165.46	62636852.42	11686.9609
31	T13F	36s	First	62621879.78	62636852.42	14972.64433
32	T14F	37s	First	62624606.71	62636852.42	12245.70835
33	T15F	36s	First	62623520.17	62636852.42	13332.24841
34	T16F	36s	First	62626239.31	62636852.42	10613.10906

35	T17F	36s	First	62625056.92	62636852.42	11795.50062
36	T18F	36s	First	62624441.5	62636852.42	12410.92023
37	T19F	36s	First	62622188.27	62636852.42	14664.14734
38	T20F	36s	First	62623180.97	62636852.42	13671.45292
39	T21F	37s	First	62622756.18	62636852.42	14096.23561
40	T22F	37s	First	62630539.81	62636852.42	6312.61203
41	T23F	37s	First	62623391.56	62636852.42	13460.85816
42	T24F	36s	First	62624135.25	62636852.42	12717.17417
43	T25F	36s	First	62626151.97	62636852.42	10700.45313
44	T01D	37s	Second	62636194.87	62636852.42	657.54975
45	T02D	37s	Second	62636462.07	62636852.42	390.35026
46	T03D	37s	Second	62635640.15	62636852.42	1212.2701
47	T04D	37s	Second	62635605.78	62636852.42	1246.64316
48	T05D	37s	Second	62635865.13	62636852.42	987.29037
49	T06D	37s	Second	62635547.74	62636852.42	1304.68047
50	T07D	37s	Second	62635806.97	62636852.42	1045.45322
51	T08D	37s	Second	62636738.32	62636852.42	114.0967
52	T09D	37s	Second	62635709	62636852.42	1143.4165
53	T10D	37s	Second	62635452.3	62636852.42	1400.11882
54	T11D	37s	Second	62636002.44	62636852.42	849.97638
55	T12D	37s	Second	62636332.81	62636852.42	519.60935
56	T13D	37s	Second	62636434.99	62636852.42	417.42773
57	T14D	37s	Second	62636701.99	62636852.42	150.42911
58	T15D	37s	Second	62636820.68	62636852.42	31.73707
59	T16D	37s	Second	62636721.37	62636852.42	131.04787
60	T17D	37s	Second	62636252.98	62636852.42	599.44097
61	T18D	37s	Second	62636247.81	62636852.42	604.61378
62	T19D	37s	Second	62635595.58	62636852.42	1256.83963
63	T20D	37s	Second	62636331.58	62636852.42	520.84416
64	T21D	37s	Second	62636637.07	62636852.42	215.34715
65	T501	36S	Second	62626445.47	62636852.42	10406.95382
66	T502	36S	Second	62626993.57	62636852.42	9858.84825
67	T503	36S	Second	62627295.18	62636852.42	9557.2389

APPENDIX 6: Extracted height anomaly (ζ_p) and Geoid undulations (N) of TAREF11 control points from TZQ17 quasi-geoid model and TZG17 geoid model

S/No	St/Name	Zone	Longitude (λ) (d.ddd)	Latitude (φ) (d.ddd)	ζ (meter)	N (meter)
1	ARIT	36s	32.82546	-5.040146	-17.52442	-18.044868
2	MOSH	37s	37.3371	-3.349947	-16.99317	-17.7527552
3	TANZ	37s	39.20793	-6.765585	-27.05221	-27.2003029
4	DARA	37s	39.29718	-6.817814	-27.4181	-27.4418333
5	ZNZB	37s	39.21072	-6.218534	-28.48417	-27.6961143
6	DODC	36s	35.7483	-6.169644	-20.21735	-19.7046485
7	T01Z	36s	34.80028	-11.27367	-18.45947	-17.7487668
8	T02Z	37s	37.34053	-11.0626	-21.91029	-22.1208433
9	T03Z	37s	40.18494	-10.33473	-25.04671	-24.7105174
10	T05Z	36S	35.75316	-7.675926	-16.2964	-17.2924189
11	T07Z	36s	31.60572	-7.951187	-10.68188	-11.3942489
12	T09Z	37s	39.11663	-5.087755	-27.26762	-27.5339167
13	T11Z	36s	32.82546	-5.04023	-17.5245	-18.0448675
14	T12Z	35s	29.66836	-4.886718	-16.76162	-15.4338733
15	T13Z	36s	31.79922	-1.325547	-14.57636	-14.7628596
16	T14Z	36S	32.92252	-2.446997	-16.60802	-17.0636508
17	T15Z	36S	33.83795	-1.53753	-17.60288	-17.4492311
18	T16Z	37s	37.80493	-6.748471	-22.76923	-22.5661125
19	T01F	36s	31.15054	-1.531898	-11.97924	-12.5594749
20	T02F	36s	34.68163	-1.834966	-16.33316	-16.7901474
21	T03F	36s	30.66942	-2.506662	-10.72335	-10.8536763
22	T04F	36s	31.36577	-2.664347	-13.19189	-13.2914801
23	T05F	36s	34.81976	-2.436597	-15.95463	-16.5642707
24	T06F	36s	35.54513	-2.067269	-15.67821	-15.8154752
25	T07F	36s	36.7041	-2.742595	-16.16528	-16.6078659
26	T08F	36s	30.70853	-3.593106	-11.96825	-12.4503107
27	T09F	36s	31.52459	-3.335702	-13.97945	-14.2184672
28	T10F	36s	32.40739	-3.405327	-16.3978	-16.7070335
29	T11F	36s	33.40612	-3.370276	-18.30727	-18.5068156
30	T12F	36s	34.30568	-3.517024	-19.40175	-19.1927935
31	T13F	36s	35.68594	-3.336089	-17.312	-17.7257829
32	T14F	37s	36.7067	-3.437632	-17.59304	-17.8323942
33	T15F	36s	30.27451	-4.480611	-12.68473	-12.7193732
34	T16F	36s	31.33704	-5.046428	-13.13627	-13.1826357

35	T17F	36s	32.86178	-4.277974	-17.27347	-17.5845963
36	T18F	36s	33.44913	-4.53164	-18.70003	-18.7626470
37	T19F	36s	34.74014	-4.813875	-17.47743	-18.2147173
38	T20F	36s	35.77196	-4.896166	-18.74682	-18.6601109
39	T21F	37s	36.93538	-4.205005	-17.87944	-17.6917020
40	T22F	37s	37.91466	-4.514897	-21.48704	-21.1203154
41	T23F	37s	38.294	-4.803467	-21.40476	-21.6286731
42	T24F	36s	30.47756	-5.614652	-11.6687	-12.624323
43	T25F	36s	31.65257	-5.328049	-13.24217	-13.3064739
44	T26F	36s	32.74393	-5.612446	-17.47354	-17.4646151
45	T27F	36s	33.15515	-5.323667	-18.3811	-18.26240708
46	T28F	36s	34.49034	-5.70068	-18.04046	-18.65331551
47	T29F	36s	35.97024	-5.967471	-19.59399	-19.29249103
48	T30F	37s	36.5778	-5.300954	-16.82243	-17.53552333
49	T31F	37s	37.28919	-5.56702	-17.61205	-18.20773844
50	T32F	37s	38.4851	-5.500057	-23.90951	-24.01522458
51	T33F	36s	30.9403	-6.36742	-12.84413	-13.11919271
52	T34F	36s	31.23707	-6.294712	-13.19433	-13.49894856
53	T35F	36s	32.06268	-6.724554	-13.25914	-13.34389232
54	T36F	36s	33.20646	-6.806987	-13.8076	-14.81275088
55	T01D	37s	39.03359	-6.580906	-26.88413	-27.08606283
56	T02D	37s	39.07509	-6.60643	-26.93763	-27.14035226
57	T03D	37s	39.16945	-6.666885	-27.10858	-27.28398282
58	T04D	37s	39.16923	-6.665853	-27.10982	-27.28525623
59	T05D	37s	39.20967	-6.766281	-27.05896	-27.20509857
60	T06D	37s	39.2068	-6.776309	-27.01941	-27.15817661
61	T07D	37s	39.19976	-6.799314	-26.92567	-27.0716556
62	T08D	37s	39.28545	-6.77839	-27.48187	-27.47437626
63	T09D	37s	39.06902	-6.696115	-26.72142	-26.94939599
64	T10D	37s	39.13736	-6.89407	-26.39061	-26.61933469
65	T11D	37s	39.16615	-6.876714	-26.55989	-26.76165525
66	T12D	37s	39.25639	-6.864195	-27.03119	-27.15596988
67	T13D	37s	39.28035	-6.943123	-26.94854	-27.13280911
68	T14D	37s	39.3533	-6.8455	-27.66119	-27.66116435

APPENDIX 7: Computed normal gravity of TAREF11 control points

S/No	St/Name	Zone	Order	Latitude φ (d.ddd)	γ_0^{GRS80} (m/s^2)	γ_Q (m/s^2)
1	ARIT	36s	CORS	-5.040146	9.780726	9.77695233
2	MOSH	37s	CORS	-3.349947	9.780503	9.777855856
3	TANZ	37s	CORS	-6.765585	9.781044	9.780742551
4	DARA	37s	CORS	-6.817814	9.781055	9.780900879
5	ZNZB	37s	CORS	-6.218534	9.780933	9.780857183
6	DODC	36s	CORS	-6.169644	9.780923	9.77746557
7	T01Z	36s	Zero	-11.27367	9.782301	9.780628002
8	T02Z	37s	Zero	-11.0626	9.782228	9.7800835
9	T03Z	37s	Zero	-10.33473	9.781989	9.781643577
10	T05Z	36S	Zero	-7.675926	9.781248	9.776841719
11	T07Z	36s	Zero	-7.951187	9.781315	9.775753868
12	T09Z	37s	Zero	-5.087755	9.780733	9.780698086
13	T11Z	36s	Zero	-5.04023	9.780726	9.776962682
14	T12Z	35s	Zero	-4.886718	9.780702	9.778155489
15	T13Z	36s	Zero	-1.325547	9.780355	9.776489442
16	T14Z	36S	Zero	-2.446997	9.780421	9.776888276
17	T15Z	36S	Zero	-1.53753	9.780364	9.77670445
18	T16Z	37s	Zero	-6.748471	9.78104	9.779486873
19	T01F	36s	First	-1.531898	9.780364	9.775278054
20	T02F	36s	First	-1.834966	9.78038	9.775391722
21	T03F	36s	First	-2.506662	9.780426	9.774910531
22	T04F	36s	First	-2.664347	9.780439	9.77600066
23	T05F	36s	First	-2.436597	9.78042	9.775783152
24	T06F	36s	First	-2.067269	9.780394	9.774149406
25	T07F	36s	First	-2.742595	9.780445	9.776345289
26	T08F	36s	First	-3.593106	9.78053	9.775963047
27	T09F	36s	First	-3.335702	9.780502	9.776715469
28	T10F	36s	First	-3.405327	9.780509	9.776619709
29	T11F	36s	First	-3.370276	9.780505	9.776730905
30	T12F	36s	First	-3.517024	9.780521	9.776830796
31	T13F	36s	First	-3.336089	9.780502	9.775776134
32	T14F	37s	First	-3.437632	9.780513	9.776647434
33	T15F	36s	First	-4.480611	9.780642	9.776433064
34	T16F	36s	First	-5.046428	9.780727	9.777376466
35	T17F	36s	First	-4.277974	9.780614	9.776891246
36	T18F	36s	First	-4.53164	9.780649	9.776731248

37	T19F	36s	First	-4.813875	9.780691	9.77606357
38	T20F	36s	First	-4.896166	9.780703	9.776386435
39	T21F	37s	First	-4.205005	9.780605	9.776153964
40	T22F	37s	First	-4.514897	9.780647	9.778653303
41	T23F	37s	First	-4.803467	9.780689	9.776438314
42	T24F	36s	First	-5.614652	9.780821	9.776809256
43	T25F	36s	First	-5.328049	9.780772	9.777394444
44	T26F	36s	First	-5.612446	9.780821	9.777187992
45	T27F	36s	First	-5.323667	9.780771	9.777026226
46	T28F	36s	First	-5.70068	9.780836	9.776811575
47	T29F	36s	First	-5.967471	9.780885	9.77758875
48	T30F	37s	First	-5.300954	9.780768	9.776016575
49	T31F	37s	First	-5.56702	9.780813	9.776911626
50	T32F	37s	First	-5.500057	9.780801	9.779576528
51	T33F	36s	First	-6.36742	9.780962	9.777759851
52	T34F	36s	First	-6.294712	9.780948	9.777206105
53	T35F	36s	First	-6.724554	9.781035	9.777386849
54	T36F	36s	First	-6.806987	9.781052	9.777363336
55	T01D	37s	Second	-6.580906	9.781005	9.780798537
56	T02D	37s	Second	-6.60643	9.78101	9.780888104
57	T03D	37s	Second	-6.666885	9.781023	9.780641041
58	T04D	37s	Second	-6.665853	9.781023	9.780629979
59	T05D	37s	Second	-6.766281	9.781044	9.780732643
60	T06D	37s	Second	-6.776309	9.781046	9.780634571
61	T07D	37s	Second	-6.799314	9.781051	9.780721275
62	T08D	37s	Second	-6.77839	9.781046	9.781010473
63	T09D	37s	Second	-6.696115	9.781029	9.780668783
64	T10D	37s	Second	-6.89407	9.781071	9.780629899
65	T11D	37s	Second	-6.876714	9.781067	9.780799696
66	T12D	37s	Second	-6.864195	9.781065	9.780900966

APPENDIX 8: Computed mean normal gravity and mean gravity of TAREF11 control points

S/No	St/Name	Zone	Order	$\bar{\gamma}$ (m/s ²)	\bar{g} (m/s ²)
1	ARIT	36s	CORS	9.775066206	9.777119676
2	MOSH	37s	CORS	9.776532586	9.777956706
3	TANZ	37s	CORS	9.780592089	9.780782866
4	DARA	37s	CORS	9.780824016	9.780931493
5	ZNZB	37s	CORS	9.780819366	9.780798267
6	DODC	36s	CORS	9.77573712	9.777869285
7	T01Z	36s	Zero	9.779791989	9.780303136
8	T02Z	37s	Zero	9.779011442	9.780222564
9	T03Z	37s	Zero	9.781470968	9.781946495
10	T05Z	36S	Zero	9.774638876	9.777794035
11	T07Z	36s	Zero	9.772973545	9.777627379
12	T09Z	37s	Zero	9.780680603	9.780308322
13	T11Z	36s	Zero	9.775081728	9.777128604
14	T12Z	35s	Zero	9.776882827	9.777991181
15	T13Z	36s	Zero	9.774557339	9.776932337
16	T14Z	36S	Zero	9.775122344	9.77720722
17	T15Z	36S	Zero	9.774875082	9.776971447
18	T16Z	37s	Zero	9.778710616	9.779647504
19	T01F	36s	First	9.778664835	9.776100137
20	T02F	36s	First	9.772897549	9.776113829
21	T03F	36s	First	9.772152731	9.776155399
22	T04F	36s	First	9.773781736	9.776787698
23	T05F	36s	First	9.773464566	9.776578947
24	T06F	36s	First	9.771026637	9.775475503
25	T07F	36s	First	9.774295408	9.777053148
26	T08F	36s	First	9.773679678	9.776752985
27	T09F	36s	First	9.774822416	9.777245782
28	T10F	36s	First	9.774675081	9.777057225
29	T11F	36s	First	9.774843751	9.777032855
30	T12F	36s	First	9.774985667	9.777107571
31	T13F	36s	First	9.773413254	9.776409895
32	T14F	37s	First	9.774714936	9.777092802
33	T15F	36s	First	9.77432859	9.777131935
34	T16F	36s	First	9.77570159	9.777962117

35	T17F	36s	First	9.775029831	9.7773331
36	T18F	36s	First	9.774772304	9.777172654
37	T19F	36s	First	9.773750026	9.776779813
38	T20F	36s	First	9.77422812	9.77689792
39	T21F	37s	First	9.773928659	9.777246301
40	T22F	37s	First	9.777656672	9.778548792
41	T23F	37s	First	9.774312986	9.778085781
42	T24F	36s	First	9.77480333	9.777568531
43	T25F	36s	First	9.775705699	9.778082618
44	T26F	36s	First	9.775371673	9.777279023
45	T27F	36s	First	9.775153702	9.777265174
46	T28F	36s	First	9.7747992	9.77722167
47	T29F	36s	First	9.775940724	9.777961816
48	T30F	37s	First	9.773640959	9.777320429
49	T31F	37s	First	9.774961062	9.777915032
50	T32F	37s	First	9.778964271	9.779904117
51	T33F	36s	First	9.776158879	9.777963279
52	T34F	36s	First	9.775335392	9.777777412
53	T35F	36s	First	9.775562878	9.778027393
54	T36F	36s	First	9.775518912	9.777931796
55	T01D	37s	Second	9.780695255	9.780652905
56	T02D	37s	Second	9.780826961	9.780751636
57	T03D	37s	Second	9.780450175	9.780600062
58	T04D	37s	Second	9.780433692	9.780588427
59	T05D	37s	Second	9.780577156	9.780772607
60	T06D	37s	Second	9.780429012	9.78069637
61	T07D	37s	Second	9.780556616	9.780811774
62	T08D	37s	Second	9.780992554	9.780967716
63	T09D	37s	Second	9.780488738	9.780684628
64	T10D	37s	Second	9.780409469	9.780751253
65	T11D	37s	Second	9.780665986	9.780927707
66	T12D	37s	Second	9.780819205	9.781016696
67	T13D	37s	Second	9.780884603	9.78107191

APPENDIX 9: Computed normal heights of TAREF11 control points using Geopotential numbers

S/No	St/Name	Zone	Order	Cp (m^2/s^2)	$\bar{\gamma}$ (m/s^2)	$H_{XGM2019e}^N$ (meter)
1	ARIT	36s	CORS	11956.78189	9.775066206	1223.191909
2	MOSH	37s	CORS	8396.22572	9.776532586	858.2142725
3	TANZ	37s	CORS	955.44781	9.780592089	97.68813598
4	DARA	37s	CORS	487.73502	9.780824016	49.86645493
5	ZNZB	37s	CORS	232.58743	9.780819366	23.7800
6	DODC	36s	CORS	10947.96787	9.77573712	1119.912262
7	T01Z	36s	Zero	5295.8293	9.779791989	541.5073558
8	T02Z	37s	Zero	6798.33851	9.779011442	695.1969072
9	T03Z	37s	Zero	1091.67555	9.781470968	111.6064806
10	T05Z	36S	Zero	13968.26045	9.774638876	1428.030845
11	T07Z	36s	Zero	17619.13327	9.772973545	1802.842624
12	T09Z	37s	Zero	113.19232	9.780680603	11.57305147
13	T11Z	36s	Zero	11924.02733	9.775081728	1219.839144
14	T12Z	35s	Zero	8053.18091	9.776882827	823.696167
15	T13Z	36s	Zero	12244.00843	9.774557339	1252.640708
16	T14Z	36S	Zero	11194.74961	9.775122344	1145.228593
17	T15Z	36S	Zero	11589.69044	9.774875082	1185.661233
18	T16Z	37s	Zero	4919.71744	9.778710616	503.1049218
19	T01F	36s	First	16115.97502	9.778664835	1648.075202
20	T02F	36s	First	15803.44549	9.772897549	1617.068573
21	T03F	36s	First	17468.55808	9.772152731	1787.585454
22	T04F	36s	First	14056.70692	9.773781736	1438.205528
23	T05F	36s	First	14693.4948	9.773464566	1503.406975
24	T06F	36s	First	19780.44175	9.771026637	2024.397485
25	T07F	36s	First	12991.34298	9.774295408	1329.13345
26	T08F	36s	First	14467.46652	9.773679678	1480.247665
27	T09F	36s	First	11994.62319	9.774822416	1227.093719
28	T10F	36s	First	12322.11233	9.774675081	1260.616054
29	T11F	36s	First	11957.58949	9.774843751	1223.302366
30	T12F	36s	First	11686.9609	9.774985667	1195.598776
31	T13F	36s	First	14972.64433	9.773413254	1531.977001
32	T14F	37s	First	12245.70835	9.774714936	1252.794422
33	T15F	36s	First	13332.24841	9.77432859	1364.00657
34	T16F	36s	First	10613.10906	9.77570159	1085.662135

35	T17F	36s	First	11795.50062	9.775029831	1206.697148
36	T18F	36s	First	12410.92023	9.774772304	1269.688934
37	T19F	36s	First	14664.14734	9.773750026	1500.360384
38	T20F	36s	First	13671.45292	9.77422812	1398.724559
39	T21F	37s	First	14096.23561	9.773928659	1442.228207
40	T22F	37s	First	6312.61203	9.777656672	645.616045
41	T23F	37s	First	13460.85816	9.774312986	1377.16668
42	T24F	36s	First	12717.17417	9.77480333	1301.015861
43	T25F	36s	First	10700.45313	9.775705699	1094.596488
44	T26F	36s	First	11507.68556	9.775371673	1177.212074
45	T27F	36s	First	11862.6507	9.775153702	1213.551322
46	T28F	36s	First	12755.52627	9.7747992	1304.93998
47	T29F	36s	First	10438.00333	9.775940724	1067.723672
48	T30F	37s	First	15054.83911	9.773640959	1540.351152
49	T31F	37s	First	12366.1939	9.774961062	1265.088814
50	T32F	37s	First	3880.01105	9.778964271	396.7711654
51	T33F	36s	First	10148.72769	9.776158879	1038.109938
52	T34F	36s	First	11853.44021	9.775335392	1212.586549
53	T35F	36s	First	11560.06478	9.775562878	1182.547228
54	T36F	36s	First	11696.63473	9.775518912	1196.523155
55	T01D	37s	Second	657.54975	9.780695255	67.22934647
56	T02D	37s	Second	390.35026	9.780826961	39.9097399
57	T03D	37s	Second	1212.2701	9.780450175	123.9482926
58	T04D	37s	Second	1246.64316	9.780433692	127.4629735
59	T05D	37s	Second	987.29037	9.780577156	100.9439785
60	T06D	37s	Second	1304.68047	9.780429012	133.3970594
61	T07D	37s	Second	1045.45322	9.780556616	106.8909737
62	T08D	37s	Second	114.0967	9.780992554	11.66514537
63	T09D	37s	Second	1143.4165	9.780488738	116.9079103
64	T10D	37s	Second	1400.11882	9.780409469	143.1554399
65	T11D	37s	Second	849.97638	9.780665986	86.90373245
66	T12D	37s	Second	519.60935	9.780819205	53.12534044
67	T13D	37s	Second	417.42773	9.780884603	42.67791176
68	T14D	37s	Second	150.42911	9.780989318	15.37974382

APPENDIX 10: Computed Normal Heights of TAREF11 control points using TZQ 17 quasi-geoid model

S/No	St/Name	Zone	Order	h^{elp} (meter)	ζ (meter)	H_{TZQ17}^N (meter)
1	ARIT	36s	CORS	1204.8501	-17.5244247	1222.374525
2	MOSH	37s	CORS	840.6029	-16.9931678	857.5960678
3	TANZ	37s	CORS	70.4607	-27.0522098	97.51290977
4	DARA	37s	CORS	22.3957	-27.4180956	49.81379557
5	ZNZB	37s	CORS	-3.9758	-28.4841682	24.5083682
6	DODC	36s	CORS	1099.9705	-20.2173525	1120.187852
7	T01Z	36s	Zero	523.3506	-18.4594685	541.8100685
8	T02Z	37s	Zero	672.8775	-21.9102888	694.7877888
9	T03Z	37s	Zero	86.8193	-25.0467094	111.8660094
10	T05Z	36S	Zero	1411.3404	-16.2963973	1428.236797
11	T07Z	36s	Zero	1791.2127	-10.6818838	1801.894584
12	T09Z	37s	Zero	-15.9371	-27.2676248	11.33052476
13	T11Z	36s	Zero	1201.4998	-17.524497	1219.024297
14	T12Z	35s	Zero	808.0352	-16.7616221	823.7968221
15	T13Z	36s	Zero	1237.5964	-14.5763646	1252.172765
16	T14Z	36S	Zero	1127.8713	-16.6080152	1144.479315
17	T15Z	36S	Zero	1167.9887	-17.6028775	1185.591577
18	T16Z	37s	Zero	480.3136	-22.7692345	503.0828345
19	T01F	36s	First	1635.7926	-11.9792356	1647.771836
20	T02F	36s	First	1599.7966	-16.3331622	1616.129762
21	T03F	36s	First	1776.2268	-10.7233538	1786.950154
22	T04F	36s	First	1424.5865	-13.1918918	1437.778392
23	T05F	36s	First	1486.4011	-15.9546333	1502.355733
24	T06F	36s	First	2007.758	-15.6782141	2023.436214
25	T07F	36s	First	1312.0802	-16.1652776	1328.245478
26	T08F	36s	First	1467.5681	-11.9682509	1479.536351
27	T09F	36s	First	1212.6474	-13.9794466	1226.626847
28	T10F	36s	First	1243.6476	-16.3977958	1260.045396
29	T11F	36s	First	1204.4967	-18.3072723	1222.803972
30	T12F	36s	First	1176.1718	-19.4017517	1195.573552
31	T13F	36s	First	1513.7447	-17.3119979	1531.056698
32	T14F	37s	First	1234.5921	-17.5930393	1252.185139
33	T15F	36s	First	1350.9344	-12.6847327	1363.619133
34	T16F	36s	First	1072.1205	-13.136268	1085.256768

35	T17F	36s	First	1188.8531	-17.2734679	1206.126568
36	T18F	36s	First	1250.6217	-18.7000278	1269.321728
37	T19F	36s	First	1481.612	-17.4774304	1499.08943
38	T20F	36s	First	1379.7599	-18.7468241	1398.506724
39	T21F	37s	First	1424.0338	-17.8794415	1441.913242
40	T22F	37s	First	624.2923	-21.4870368	645.7793368
41	T23F	37s	First	1355.7271	-21.4047569	1377.131857
42	T24F	36s	First	1288.0956	-11.6687008	1299.764301
43	T25F	36s	First	1081.0007	-13.2421746	1094.242875
44	T26F	36s	First	1159.4327	-17.4735373	1176.906237
45	T27F	36s	First	1194.9442	-18.3811006	1213.325301
46	T28F	36s	First	1285.9025	-18.040462	1303.942962
47	T29F	36s	First	1048.2643	-19.5939864	1067.858286
48	T30F	37s	First	1522.4865	-16.8224276	1539.308928
49	T31F	37s	First	1246.2798	-17.612054	1263.891854
50	T32F	37s	First	372.8097	-23.9095063	396.7192063
51	T33F	36s	First	1024.525	-12.844134	1037.369134
52	T34F	36s	First	1198.957	-13.1943304	1212.15133
53	T35F	36s	First	1168.6051	-13.2591417	1181.864242
54	T36F	36s	First	1181.3096	-13.8076039	1195.117204
55	T01D	37s	Second	40.0517	-26.8841279	66.93582793
56	T02D	37s	Second	12.6886	-26.9376321	39.62623211
57	T03D	37s	Second	96.5896	-27.1085772	123.6981772
58	T04D	37s	Second	100.1017	-27.1098192	127.2115192
59	T05D	37s	Second	73.7106	-27.0589625	100.7695625
60	T06D	37s	Second	106.2005	-27.0194064	133.2199064
61	T07D	37s	Second	79.7877	-26.9256733	106.7133733
62	T08D	37s	Second	-15.8684	-27.4818721	11.61347215
63	T09D	37s	Second	89.9635	-26.721423	116.684923
64	T10D	37s	Second	116.4669	-26.3906123	142.8575123
65	T11D	37s	Second	60.096	-26.5598885	86.65588849
66	T12D	37s	Second	25.9569	-27.0311885	52.98808853
67	T13D	37s	Second	15.5828	-26.9485442	42.53134417
68	T14D	37s	Second	-12.2723	-27.6611925	15.38889252

APPENDIX 11: Computed Normal Heights of TAREF11 control points using a strict formula for geoid to quasi-geoid separation

S/No	St/Name	Zone	N- ζ (meter)	ζ (meter)	h^{elp} (meter)	H_{SGQS}^N (meter)
1	ARIT	36s	-0.313	-18.358	1204.850	1223.208
2	MOSH	37s	-0.135	-17.887	840.603	858.490
3	TANZ	37s	0.011	-27.189	70.461	97.650
4	DARA	37s	0.006	-27.436	22.396	49.831
5	ZNZB	37s	0.003	-27.693	-3.976	23.717
6	DODC	36s	-0.229	-19.934	1099.971	1119.904
7	T01Z	36s	-0.044	-17.793	523.351	541.144
8	T02Z	37s	-0.051	-22.172	672.878	695.050
9	T03Z	37s	0.016	-24.695	86.819	111.514
10	T05Z	36s	-0.370	-17.663	1411.340	1429.003
11	T07Z	36s	-0.553	-11.947	1791.213	1803.160
12	T09Z	37s	0.001	-27.533	-15.937	11.596
13	T11Z	36s	-0.312	-18.356	1201.500	1219.856
14	T12Z	35s	-0.131	-15.565	808.035	823.601
15	T13Z	36s	-0.301	-15.064	1237.596	1252.660
16	T14Z	36s	-0.245	-17.309	1127.871	1145.180
17	T15Z	36s	-0.292	-17.741	1167.989	1185.730
18	T16Z	37s	-0.005	-22.571	480.314	502.884
19	T01F	36s	-0.538	-13.097	1635.793	1648.890
20	T02F	36s	-0.556	-17.346	1599.797	1617.143
21	T03F	36s	-0.599	-11.453	1776.227	1787.680
22	T04F	36s	-0.397	-13.689	1424.587	1438.275
23	T05F	36s	-0.441	-17.006	1486.401	1503.407
24	T06F	36s	-0.828	-16.643	2007.758	2024.401
25	T07F	36s	-0.317	-16.925	1312.080	1329.005
26	T08F	36s	-0.426	-12.876	1467.568	1480.444
27	T09F	36s	-0.283	-14.501	1212.647	1227.149
28	T10F	36s	-0.334	-17.042	1243.648	1260.689
29	T11F	36s	-0.315	-18.822	1204.497	1223.319
30	T12F	36s	-0.302	-19.495	1176.172	1195.666
31	T13F	36s	-0.486	-18.211	1513.745	1531.956
32	T14F	37s	-0.297	-18.130	1234.592	1252.722
33	T15F	36s	-0.358	-13.077	1350.934	1364.012

34	T01D	37s	0.007	-27.079	40.052	67.131
35	T02D	37s	0.004	-27.136	12.689	39.825
36	T03D	37s	0.013	-27.271	96.590	123.860
37	T04D	37s	0.013	-27.272	100.102	127.374
38	T05D	37s	0.012	-27.193	73.711	100.904
39	T06D	37s	0.015	-27.143	106.201	133.344
40	T07D	37s	0.012	-27.059	79.788	106.847
41	T08D	37s	0.002	-27.473	-15.868	11.604
42	T09D	37s	0.012	-26.938	89.964	116.901
43	T10D	37s	0.016	-26.604	116.467	143.070
44	T11D	37s	0.011	-26.751	60.096	86.847
45	T12D	37s	0.007	-27.149	25.957	53.106
46	T13D	37s	0.006	-27.127	15.583	42.710
47	T14D	37s	0.002	-27.659	-12.272	15.387
48	T15D	37s	0.001	-27.894	-24.663	3.231
49	T001	36s	-0.547	-11.870	1649.615	1661.485
50	T002	36s	-0.338	-12.552	1235.665	1248.216
51	T003	36s	-0.274	-13.654	1143.072	1156.725
52	T004	36s	-0.305	-15.021	1211.891	1226.911
53	T005	36s	-0.433	-12.319	1440.972	1453.291
54	T006	36s	-0.326	-15.075	1313.907	1328.982
55	T007	36s	-0.484	-12.798	1551.334	1564.132
56	T008	36s	-0.331	-15.052	1275.425	1290.476
57	T011	36s	-0.254	-17.316	1169.162	1186.477
58	T012	36s	-0.257	-17.584	1136.460	1154.044
59	T013	36s	-0.313	-17.837	1225.462	1243.299
60	T014	36s	-0.385	-17.809	1347.438	1365.247
61	T020	36s	-0.287	-17.619	1178.976	1196.595
62	T021	36s	-0.418	-16.934	1406.646	1423.580
63	T022	36s	-0.313	-17.541	1226.150	1243.691
64	T023	36s	-0.368	-16.716	1311.838	1328.554
65	T024	36s	-0.352	-17.576	1274.478	1292.054
66	T025	36s	-0.412	-17.884	1405.506	1423.389

APPENDIX 12: Computed orthometric height of TAREF11 control points using Geopotential number

S/No	St/Name	Zone	Order	Cp (m^2/s^2)	\bar{g} (m/s^2)	$H_{XGM2019e}^0$ (meter)
1	ARIT	36s	CORS	11956.78189	9.777119676	1222.935004
2	MOSH	37s	CORS	8396.22572	9.777956706	858.6891896
3	TANZ	37s	CORS	955.44781	9.780782866	97.68623055
4	DARA	37s	CORS	487.73502	9.780931493	49.86590698
5	ZNZB	37s	CORS	232.58743	9.780798267	23.78000483
6	DODC	36s	CORS	10947.96787	9.777869285	1119.668053
7	T01Z	36s	Zero	5295.8293	9.780303136	541.479055
8	T02Z	37s	Zero	6798.33851	9.780222564	695.1108183
9	T03Z	37s	Zero	1091.67555	9.781946495	111.6010551
10	T05Z	36S	Zero	13968.26045	9.777794035	1428.569716
11	T07Z	36s	Zero	17619.13327	9.777627379	1801.984529
12	T09Z	37s	Zero	113.19232	9.780308322	11.57349199
13	T11Z	36s	Zero	11924.02733	9.777128604	1219.583767
14	T12Z	35s	Zero	8053.18091	9.777991181	823.6027995
15	T13Z	36s	Zero	12244.00843	9.776932337	1252.336419
16	T14Z	36S	Zero	11194.74961	9.77720722	1144.984386
17	T15Z	36S	Zero	11589.69044	9.776971447	1185.407005
18	T16Z	37s	Zero	4919.71744	9.779647504	503.0567245
19	T01F	36s	First	16115.97502	9.776100137	1648.507564
20	T02F	36s	First	15803.44549	9.776113829	1616.536567
21	T03F	36s	First	17468.55808	9.776155399	1786.85356
22	T04F	36s	First	14056.70692	9.776787698	1437.763338
23	T05F	36s	First	14693.4948	9.776578947	1502.928057
24	T06F	36s	First	19780.44175	9.775475503	2023.476172
25	T07F	36s	First	12991.34298	9.777053148	1328.758552
26	T08F	36s	First	14467.46652	9.776752985	1479.782351
27	T09F	36s	First	11994.62319	9.777245782	1226.789574
28	T10F	36s	First	12322.11233	9.777057225	1260.30891
29	T11F	36s	First	11957.58949	9.777032855	1223.028466
30	T12F	36s	First	11686.9609	9.777107571	1195.339298
31	T13F	36s	First	14972.64433	9.776409895	1531.507424
32	T14F	37s	First	12245.70835	9.777092802	1252.489733
33	T15F	36s	First	13332.24841	9.777131935	1363.615475
34	T16F	36s	First	10613.10906	9.777962117	1085.411145

35	T17F	36s	First	11795.50062	9.7773331	1206.412884
36	T18F	36s	First	12410.92023	9.777172654	1269.377219
37	T19F	36s	First	14664.14734	9.776779813	1499.895428
38	T20F	36s	First	13671.45292	9.77689792	1398.342606
39	T21F	37s	First	14096.23561	9.777246301	1441.738827
40	T22F	37s	First	6312.61203	9.778548792	645.5571439
41	T23F	37s	First	13460.85816	9.778085781	1376.635311
42	T24F	36s	First	12717.17417	9.777568531	1300.64792
43	T25F	36s	First	10700.45313	9.778082618	1094.330407
44	T26F	36s	First	11507.68556	9.777279023	1176.982423
45	T27F	36s	First	11862.6507	9.777265174	1213.289247
46	T28F	36s	First	12755.52627	9.77722167	1304.616659
47	T29F	36s	First	10438.00333	9.777961816	1067.502975
48	T30F	37s	First	15054.83911	9.777320429	1539.771476
49	T31F	37s	First	12366.1939	9.777915032	1264.706623
50	T32F	37s	First	3880.01105	9.779904117	396.7330358
51	T33F	36s	First	10148.72769	9.777963279	1037.918368
52	T34F	36s	First	11853.44021	9.777777412	1212.283703
53	T35F	36s	First	11560.06478	9.778027393	1182.249171
54	T36F	36s	First	11696.63473	9.777931796	1196.227891
55	T01D	37s	Second	657.54975	9.780652905	67.22963757
56	T02D	37s	Second	390.35026	9.780751636	39.91004726
57	T03D	37s	Second	1212.2701	9.780600062	123.9463931
58	T04D	37s	Second	1246.64316	9.780588427	127.4609569
59	T05D	37s	Second	987.29037	9.780772607	100.9419613
60	T06D	37s	Second	1304.68047	9.78069637	133.393413
61	T07D	37s	Second	1045.45322	9.780811774	106.8881852
62	T08D	37s	Second	114.0967	9.780967716	11.66517499
63	T09D	37s	Second	1143.4165	9.780684628	116.9055688
64	T10D	37s	Second	1400.11882	9.780751253	143.1504374
65	T11D	37s	Second	849.97638	9.780927707	86.90140705
66	T12D	37s	Second	519.60935	9.781016696	53.12426777
67	T13D	37s	Second	417.42773	9.78107191	42.67709448

APPENDIX 13: Computed orthometric height of TAREF11 control points using TZG17 geoid model

S/No	St/Name	Zone	Order	h^{elp} (meter)	N (meter)	H_{TZG17}^0 (meter)
1	ARIT	36s	CORS	1204.8501	-18.0448685	1222.894968
2	MOSH	37s	CORS	840.6029	-17.7527552	858.3556552
3	TANZ	37s	CORS	70.4607	-27.200303	97.66100295
4	DARA	37s	CORS	22.3957	-27.4418333	49.8375333
5	ZNZB	37s	CORS	-3.9758	-27.6961144	23.72031439
6	DODC	36s	CORS	1099.9705	-19.7046485	1119.675149
7	T01Z	36s	Zero	523.3506	-17.7487668	541.0993668
8	T02Z	37s	Zero	672.8775	-22.1208433	694.9983433
9	T03Z	37s	Zero	86.8193	-24.7105174	111.5298174
10	T05Z	36S	Zero	1411.3404	-17.292419	1428.632819
11	T07Z	36s	Zero	1791.2127	-11.394249	1802.606949
12	T09Z	37s	Zero	-15.9371	-27.5339168	11.59681679
13	T11Z	36s	Zero	1201.4998	-18.0448675	1219.544668
14	T12Z	35s	Zero	808.0352	-15.4338733	823.4690733
15	T13Z	36s	Zero	1237.5964	-14.7628596	1252.35926
16	T14Z	36S	Zero	1127.8713	-17.0636509	1144.934951
17	T15Z	36S	Zero	1167.9887	-17.4492311	1185.437931
18	T16Z	37s	Zero	480.3136	-22.5661126	502.8797126
19	T01F	36s	First	1635.7926	-12.559475	1648.352075
20	T02F	36s	First	1599.7966	-16.7901474	1616.586747
21	T03F	36s	First	1776.2268	-10.8536763	1787.080476
22	T04F	36s	First	1424.5865	-13.2914801	1437.87798
23	T05F	36s	First	1486.4011	-16.5642707	1502.965371
24	T06F	36s	First	2007.758	-15.8154753	2023.573475
25	T07F	36s	First	1312.0802	-16.607866	1328.688066
26	T08F	36s	First	1467.5681	-12.4503108	1480.018411
27	T09F	36s	First	1212.6474	-14.2184672	1226.865867
28	T10F	36s	First	1243.6476	-16.7070336	1260.354634
29	T11F	36s	First	1204.4967	-18.5068156	1223.003516
30	T12F	36s	First	1176.1718	-19.1927936	1195.364594
31	T13F	36s	First	1513.7447	-17.725783	1531.470483
32	T14F	37s	First	1234.5921	-17.8323943	1252.424494
33	T15F	36s	First	1350.9344	-12.7193733	1363.653773

34	T16F	36s	First	1072.1205	-13.1826357	1085.303136
35	T17F	36s	First	1188.8531	-17.5845963	1206.437696
36	T18F	36s	First	1250.6217	-18.7626471	1269.384347
37	T19F	36s	First	1481.612	-18.2147173	1499.826717
38	T20F	36s	First	1379.7599	-18.660111	1398.420011
39	T21F	37s	First	1424.0338	-17.6917021	1441.725502
40	T22F	37s	First	624.2923	-21.1203155	645.4126155
41	T23F	37s	First	1355.7271	-21.6286732	1377.355773
42	T24F	36s	First	1288.0956	-12.6243235	1300.719924
43	T25F	36s	First	1081.0007	-13.306474	1094.307174
44	T26F	36s	First	1159.4327	-17.4646152	1176.897315
45	T27F	36s	First	1194.9442	-18.2624071	1213.206607
46	T28F	36s	First	1285.9025	-18.6533155	1304.555816
47	T29F	36s	First	1048.2643	-19.292491	1067.556791
48	T30F	37s	First	1522.4865	-17.5355233	1540.022023
49	T31F	37s	First	1246.2798	-18.2077384	1264.487538
50	T32F	37s	First	372.8097	-24.0152246	396.8249246
51	T33F	36s	First	1024.525	-13.1191927	1037.644193
52	T34F	36s	First	1198.957	-13.4989486	1212.455949
53	T35F	36s	First	1168.6051	-13.3438923	1181.948992
54	T36F	36s	First	1181.3096	-14.8127509	1196.122351
55	T01D	37s	Second	40.0517	-27.0860628	67.13776283
56	T02D	37s	Second	12.6886	-27.1403523	39.82895226
57	T03D	37s	Second	96.5896	-27.2839828	123.8735828
58	T04D	37s	Second	100.1017	-27.2852562	127.3869562
59	T05D	37s	Second	73.7106	-27.2050986	100.9156986
60	T06D	37s	Second	106.2005	-27.1581766	133.3586766
61	T07D	37s	Second	79.7877	-27.0716556	106.8593556
62	T08D	37s	Second	-15.8684	-27.4743763	11.60597626
63	T09D	37s	Second	89.9635	-26.949396	116.912896
64	T10D	37s	Second	116.4669	-26.6193347	143.0862347
65	T11D	37s	Second	60.096	-26.7616553	86.85765525
66	T12D	37s	Second	25.9569	-27.1559699	53.11286988

APPENDIX 14: Computed dynamic height of TAREF11 control points using Geopotential number

S/No	St/Name	Zone	Order	C_p (m^2/s^2)	γ_Q (m/s^2)	H^D (meter)
1	ARIT	36s	CORS	11956.78189	9.802429328	1219.777413
2	MOSH	37s	CORS	8396.22572	9.803554302	856.447107
3	TANZ	37s	CORS	955.44781	9.805899009	97.43602388
4	DARA	37s	CORS	487.73502	9.806046179	49.73819326
5	ZNZB	37s	CORS	232.58743	9.806124257	23.7185889
6	DODC	36s	CORS	10947.96787	9.802744451	1116.826816
7	T01Z	36s	Zero	5295.8293	9.804528338	540.141159
8	T02Z	37s	Zero	6798.33851	9.804056463	693.4209871
9	T03Z	37s	Zero	1091.67555	9.805854724	111.328954
10	T05Z	36S	Zero	13968.26045	9.801796385	1425.071477
11	T07Z	36s	Zero	17619.13327	9.800642487	1797.752881
12	T09Z	37s	Zero	113.19232	9.806164917	11.54297536
13	T11Z	36s	Zero	11924.02733	9.802439659	1216.434658
14	T12Z	35s	Zero	8053.18091	9.803655464	821.4467491
15	T13Z	36s	Zero	12244.00843	9.802337439	1249.090689
16	T14Z	36S	Zero	11194.74961	9.80266954	1142.010303
17	T15Z	36S	Zero	11589.69044	9.802542758	1182.314704
18	T16Z	37s	Zero	4919.71744	9.804647802	501.7740096
19	T01F	36s	First	16115.97502	9.801117649	1644.299722
20	T02F	36s	First	15803.44549	9.801215205	1612.396541
21	T03F	36s	First	17468.55808	9.80068856	1782.380694
22	T04F	36s	First	14056.70692	9.801765114	1434.099548
23	T05F	36s	First	14693.4948	9.801565998	1499.096655
24	T06F	36s	First	19780.44175	9.799959534	2018.420758
25	T07F	36s	First	12991.34298	9.802102859	1325.36285
26	T08F	36s	First	14467.46652	9.801636358	1476.025634
27	T09F	36s	First	11994.62319	9.802416215	1223.63945
28	T10F	36s	First	12322.11233	9.802313162	1257.061688
29	T11F	36s	First	11957.58949	9.802428004	1219.859966
30	T12F	36s	First	11686.9609	9.802511975	1192.24143
31	T13F	36s	First	14972.64433	9.801477505	1527.590542
32	T14F	37s	First	12245.70835	9.802337401	1249.264114
33	T15F	36s	First	13332.24841	9.801993782	1360.156791

34	T16F	36s	First	10613.10906	9.802852175	1082.655218
35	T17F	36s	First	11795.50062	9.802479432	1203.318069
36	T18F	36s	First	12410.92023	9.802284557	1266.125275
37	T19F	36s	First	14664.14734	9.801576069	1496.100957
38	T20F	36s	First	13671.45292	9.801886206	1394.777763
39	T21F	37s	First	14096.23561	9.801752365	1438.134232
40	T22F	37s	First	6312.61203	9.804207631	643.8676401
41	T23F	37s	First	13460.85816	9.801952116	1373.283403
42	T24F	36s	First	12717.17417	9.802190683	1297.380818
43	T25F	36s	First	10700.45313	9.802824463	1091.568371
44	T26F	36s	First	11507.68556	9.802569541	1173.945822
45	T27F	36s	First	11862.6507	9.802457233	1210.171125
46	T28F	36s	First	12755.52627	9.802177798	1301.295134
47	T29F	36s	First	10438.00333	9.802905831	1064.786657
48	T30F	37s	First	15054.83911	9.801452061	1535.980487
49	T31F	37s	First	12366.1939	9.802301301	1261.560272
50	T32F	37s	First	3880.01105	9.804975917	395.7185701
51	T33F	36s	First	10148.72769	9.802999859	1035.267554
52	T34F	36s	First	11853.44021	9.802460854	1209.231068
53	T35F	36s	First	11560.06478	9.802554252	1179.291079
54	T36F	36s	First	11696.63473	9.802513383	1193.228132
55	T01D	37s	Second	657.54975	9.80599335	67.05590413
56	T02D	37s	Second	390.35026	9.806077612	39.80697231
57	T03D	37s	Second	1212.2701	9.805818218	123.6276334
58	T04D	37s	Second	1246.64316	9.805807379	127.1331479
59	T05D	37s	Second	987.29037	9.805888961	100.6834132
60	T06D	37s	Second	1304.68047	9.805788841	133.0520666
61	T07D	37s	Second	1045.45322	9.805870622	106.615033
62	T08D	37s	Second	114.0967	9.806164044	11.63520205